Synthesis, Conformation, and Chemical Properties of New Mini Parallel Double-Stranded Peptides Conjugated with –Phe–Phe– and –Phe–Phe–X– Sequences

Shigeki KOBAYASHI,*[,a] Hiroki KOBAYASHI,[a] Takatoshi YAMAGUCHI,[a] Miharu NISHIDA,[a] Kentaro YAMAGUCHI,[b] Masaaki KURIHARA,[c] Naoki MIYATA,[c] and Akira TANAKA*[,a]

Department of Analytical Chemistry of Medicines, Showa Pharmaceutical University,[a] 3–3165 Higashi-Tamagawagakuen, Machida, Tokyo 194–8543, Japan, Chemical Analysis Center, Chiba Univercity,[b] 1–33 Yayoicho, Inage-ku, Chiba 263–8522, Japan, and Division of Organic Chemistry, National Institute of Health Sciences,[c] 1–18–1 Kamiyoga, Setagaya-ku, Tokyo 158–8501, Japan. Received December 6, 1999; accepted March 4, 2000

To investigate the chemical conformations and functions of the –Phe–Phe–Val– or –Phe–Phe– sequences contained in the Alzheimer's disease related β-amyloid peptide, a series of mini parallel double-stranded peptides conjugated with two peptide residues to one spacer were designed and prepared. The structure of the compounds was elucidated by circular dichroism (CD) spectrum and NMR two dimensional (2D) nuclear Overhauser enhancement and exchange spectroscopy (NOESY) measurments. The structure of 1,2-ethano-bis(L-Phe–L-Phe–L-Leu), 1,12-dodecano-bis(L-Phe–L-Phe–L-Leu), 1,12-dodecano-bis(L-Phe–L-Phe–L-Val), and 1,12-dodecano (D-Phe–D-Phe–D-Leu) conjugated with L-Leu and L-Val residues show a β-turn-like nucleation. The dihedral angles ($\theta=+75°$, $+180°$, $\omega=+90°$, $\phi=-87°$, $\psi=+180°$) obtained from experimental coupling constant (J) data, *etc.* support that 1,12-dodecano-bis(L-Phe–L-Phe) adopts β-turn mimic nucleation. The 1,12-dodecano-bis(L-Leu–L-Leu–L-Phe), 1,12-dodecano-bis(L-Ile–L-Phe–L-Leu), and 1,12-dodecano-bis(L-Phe–L-Val–L-Leu), *etc.* adopt most probably a random structure by CD studies.

It was found by titration spectrum that an inclusion complex of 1 : 1 ratio (association constant; $K_a=1.0\times10^4\,M^{-1}$) is formed between 1,12-dodecano-bis(L-Phe–L-Phe–L-Leu) and azobenzene (guest, $[L_0]=1.758\times10^{-5}\,M^{-1}$). Moreover, the stability of the complexes was increased in order of 1,12-dodecano-bis(L-Phe–L-Phe–L-Leu)·azobenzene>1,12-dodecano-bis(L-Phe–L-Phe–L-Val)·azobenzene>1,12-dodecano-bis(L-Phe–L-Val–L-Leu)·azobenzene. The data show that X–Phe–L-Phe–L-spacer(S)–L-Phe–L-Phe–X (X=amino acids; S=1,2-ethano- and 1,12-dodecano-) plays an important role as a binding site of the artificial receptor. The hydrophobic interaction of the four Phes in the two strands is a very interesting issue in the physiological action of proteins as well as the conformation of the backbone of X-L-Phe–L-Phe–spacer(S)–L-Phe–L-Phe–X.

Key words double-stranded peptide; β-turn mimetics; β-amyloid peptide; binding affinity; artificial receptor; downfield shift

Much attention has been paid by chemists to the mechanisms of β-sheet folding and the functions of β-sheet structures found in peptides and proteins. However, their functions are poorly understood yet in comparison with α-helical structures.[1] The heptad repeat unit –Pro–X–X– segment found in gene regulatory proteins,[2] the –Phe–Phe–Val– sequence contained in Alzheimer's disease related β-amyloid peptide,[3] the two β-strands of the DNA recognition motif of the *met* repressor protein dimer,[4] and the repeat unit –Pro–Val–Orn–Leu–D-Phe– found in antibacterial gramicidins S,[5] *etc.* are given as examples of β-turn and antiparallel β-sheet structures in living body. The type II′ β-turn conformation adopted by the –Pro–X–X– segment can stabilize a β-turn conformation, and the –Pro–Val–Orn–Leu–D-Phe– sequence of gramicidins S adopts a stable antiparallel β-sheet structure. To clarify the chemical stability, functions, and stereochemistry of β-turn (or β-hairpin) and antiparallel β-sheet structures, recently, the design and synthesis of peptides have been reported by a number of research groups.[6] The model compounds which mimic β-sheet and β-turn structures have been shown to adopt β-hairpin structures in aqueous solution, and that hydrogen bonding can stabilize β-turn structures.

This paper deals with the stereochemistry and chemical properties of the –Phe–Phe–Val– sequence contained in Alzheimer's disease related β-amyloid peptide, since the conformation, stability, and biological role of its hydrophobic sequence are poorly understood. First, we investigated the conformation and stability of parallel double-stranded peptides which consist of two parallel strands of –Phe–Phe–Val– conjugated by a mini loop. The conformation change was studied in the cases of the replacement of –Phe–Phe–Val– in –Phe–Phe–Leu– and of –Phe–Phe–Val– in –Phe–Phe–, *etc.* The design and synthesis of double-stranded peptides, *e.g.* 1,2-ethano-bis(AA)s and 1,12-dodecano-bis(AA)s (AA= amino acids) **1**—**3**, were studied as a model of simple mini parallel β-turn-like peptide mimetics, as shown in Chart 1. Compounds **1**—**3** contain a parallel double-stranded peptide sequence conjugated with a spacer, such as an ethano- or dodecano-group in geometrical symmetry, and changes in the tertiary conformation can be expected from species of the amino acid residues or spacers. The conformation of parallel double-stranded peptides was analyzed by using both experimental and computational approaches. Studies by ^{1}H-NMR titrations, nuclear Overhauser effects (NOE), and circular dichroism (CD) spectrum measurements revealed the structure of the parallel 1,2-ethano-bis(L-Phe–L-Phe) and 1,12-dodecano-bis(L-Phe–L-Phe), *etc.* which mediate a β-turn sheet nucleation.

The CD spectra of the 1,2-ethano-bis(L-Phe–L-Phe–L-Leu), 1,12-dodecano-bis(L-Phe–L-Phe–L-Leu), and 1,12-dodecano-bis(L-Phe–L-Phe–L-Val) conjugated L-Leu and L-Val residues show β-sheet nucleation. On the other hand, it is clear that the conformation of 1,12-dodecano-bis(L-Leu–L-Leu–L-Phe)

* To whom correspondence should be addressed. e-mail: kobayasi@ac.shoyaku.ac.jp

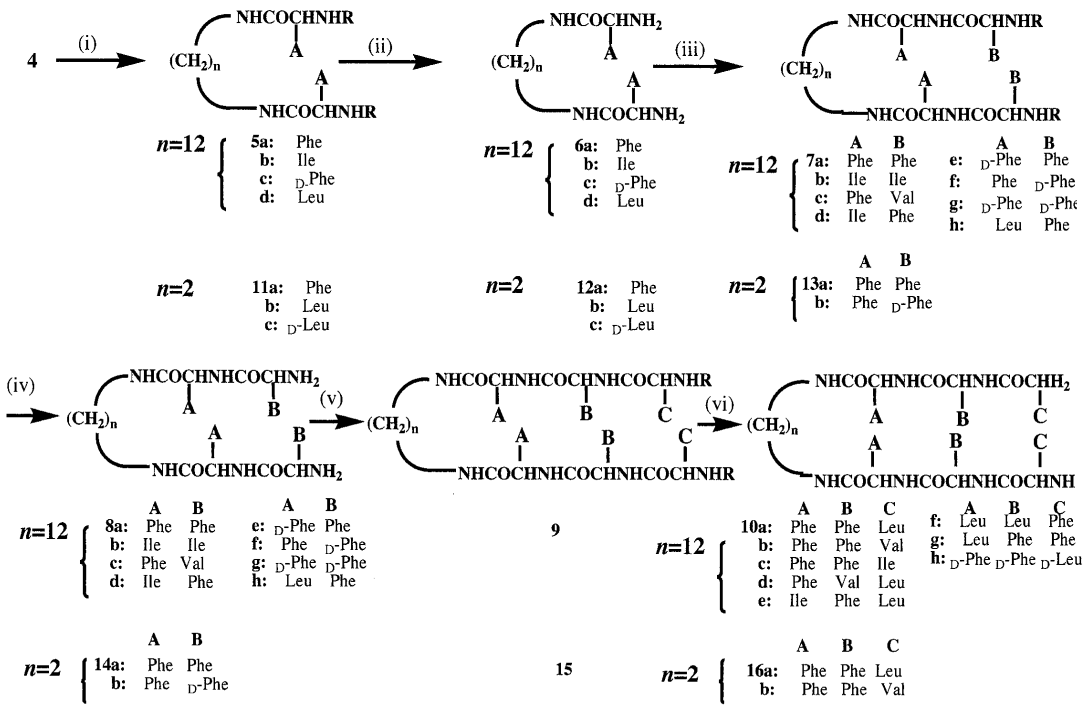

Chart 1. Pathway for the Synthesis of Mini Parallel Double-Stranded Peptides Corresponding to Peptides **1**—**3**

(i) CDI, ZAOH, dry $CHCl_3$. (ii) 5% Pd/C, H_2, DMF CH_3OH (or TFA at 4 °C). (iii) CDI, ZBOH, dry $CHCl_3$ (or DEPC, ZBOH, TEA, DMF). (iv) 5% Pd/C, H_2, DMF/CH_3OH (or TFA). (v) CDI, ZCOH, dry $CHCl_3$ (or DEPC, ZCOH, TEA, DMF). (vi) 5% Pd/C, H_2, DMF CH_3OH (or TFA at 4 °C). Where A—C represent the corresponding amino acid residues.

and 1,12-dodecano-bis(L-Ile–L-Phe–L-Leu), *etc.* probably adopts a random structure by CD spectrum and two dimensional (2D) nuclear Overhauser enhancement and exchange spectroscopy (NOESY) experiments. We show four dihedral angles (ω, ϕ, ψ, θ) obtained from the data of NMR NOEs, $^3J_{C\alpha H,NH}$ coupling constants and molecular mechanics (MM2)[7] calculation. The average dihedral angles at $\omega=-70°$, $\phi=-89°$, $\psi=+115°$, and $\theta=+75°$ (and $+180°$) support that the backbone of 1,12-dodecano-bis(L-Phe–L-Phe) is a nucleation mediated β-turn sheet. The $-^1$Phe–^{2}Phe– residues on parallel double-stranded act as a hydrophobic connector to stabilize a turn conformation mediated β-sheet nucleation. The data for the binding affinity (K_a) between ligand and double-stranded peptides also indicate that the X–Phe–L-Phe–L–spacer(S)–L-Phe–L-Phe–X (X=Val, Ile, Leu; S=ethano-, dodecano-) adopt the β-turn sheet structure and that the compounds are useful artificial receptor models. It seems that the synthesis of X–Phe–L-Phe–L–spacer(S)–L-Phe–L-Phe–X conjugated spacer to the –Phe–Phe–Val– sequence contained in Alzheimer's disease related β-amyloid peptide can contribute to the development of useful agents for elucidating the structures and chemical functions of –Phe–Phe–Val– and –Phe–Phe– analoges, *etc.*

Results and Discussion

Synthesis of Double-Stranded Peptides and Assignment of Chemical Shifts Three different types of C_2 symmetrical double-stranded peptides **1**—**3** were synthesized. The syntheses of 1,2-ethano-bis(peptide) and 1,12-dodecano-bis(peptide) **1**—**3** conjugated with a spacer such as ethylenediamine or 1,12-dodecanodiamine(**4**) at the C-terminal of the amino acid residues were carried out by stepwise condensation followed by coupling of carbobenzoxy protected-L-amino acid (CbzPheOH, Cbz=carbobenzoxy) with the spacer, as shown in Chart 1. The couplings were carried out by the C-activating method using *N,N'*-carbonyldiimidazole (CDI)[8] in dry chloroform (or the diethyl phosphoro cyanidate (DEPC) method[9] in dry dimethylformamide (DMF)). By coupling Cbz-L-LeuOH and **8a** using CDI, we obtained the 1,12-dodecano-bis(L-Phe–L-Phe–L-LeuCbz) **9a**. The target **10a** (1,12-dodecano-bis(L-Phe–L-Phe–L-Leu)) was obtained by controlled hydrogenation over Pd/C mild catalytic deprotection of **9a** in DMF/MeOH in an overall yield of 58.5%. To form a different configuration in these compounds, the D-Phe residue was introduced, and **6c** and **8e** were obtained as the enantiomer and diastereomer for **6a** and **8a**, respectively. The *tert*-butyloxycarbonyl group (=Boc) was used for N protection of D-Phe and removed with trifluoroacetic acid (TFA) to produce 1,2-ethano-bis(L-Phe–D-Phe), 1,12-dodecano-bis(D-Phe–D-Phe), and 1,2-ethano-bis(L-Phe–L-Phe–L-Leu), *etc.*

All free bases were purified in an overall yield of 40—60% after recrystallization and by silica gel column chromatography or by reverse-phase high performance liquid chromatography (RP-HPLC), and characterized by ^{1}H- and ^{13}C-NMR, IR spectrometry, FAB mass spectrometry, and/or elemental analysis. The purity of these double-stranded peptides was checked by thin layer chromatography (TLC) or analytical RP-HPLC. The samples were dissolved in MeOH and loaded on a 5×150 mm Octadecylsilane (ODS) C18 column, and were eluted with 90% acetonitrile containing 0.05% TFA at room temperature. In order to demonstrate the effect of the secondary structure formation of parallel double-stranded peptides, we synthesized single-stranded peptides **17a**, **18a**, and **19a**, as shown in Chart 2. The synthesis was performed by stepwise reactions of, for example, lauryl-

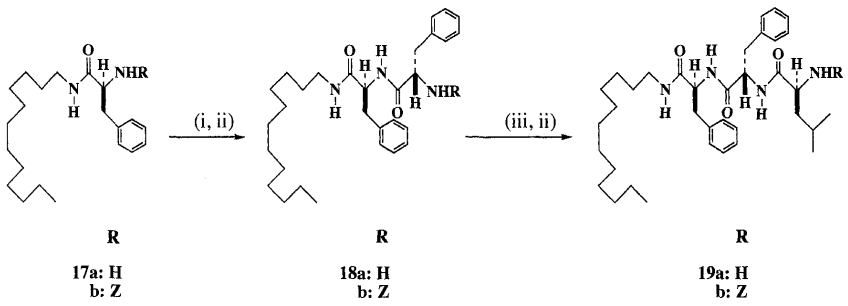

Chart 2. Pathway of the Synthesis of Single-Stranded Peptides Conjugated with a Spacer
(i) CDI, ZPheOH, dry $CHCl_3$. (ii) 5% Pd/C, H_2, CH_3OH. (iii) CDI, ZLeuOH, dry $CHCl_3$.

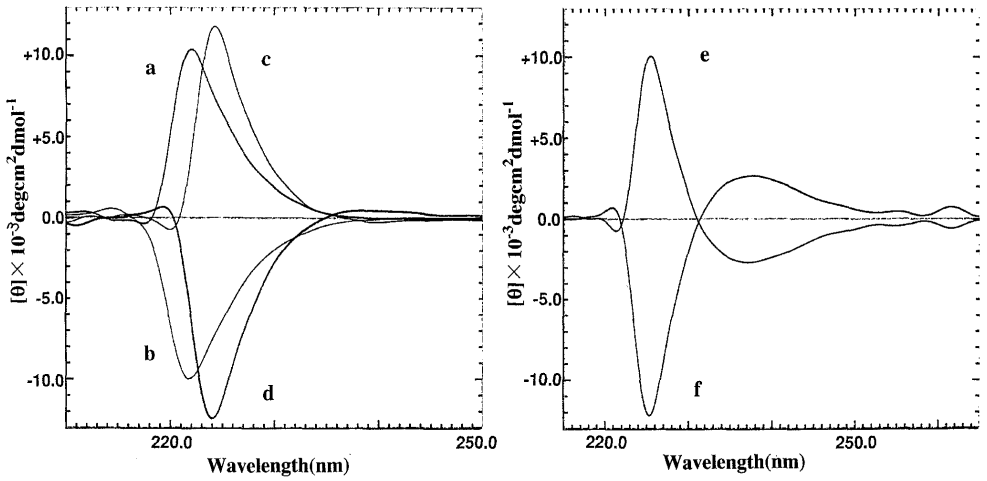

Fig. 1. CD Spectra for Mirror Images of Double-Stranded Peptides, **6a**, **6c**, **8a**, **8g**, **10a** and **10h**
Double-stranded peptides concentration, **6a** (1.05×10^{-3} M) (a), **6c** (1.21×10^{-3} M) (b), **8a** (6.91×10^{-4} M) (c), **8g** (7.28×10^{-4} M) (d), **10a** (5.52×10^{-4} M) (e) and **10h** (5.23×10^{-4} M) (f) in 85 % methanol at 22 °C, *x*-axis, nm; *y*-axis, molar ellipticity [θ].

amine with the corresponding amino acid residue employing CDI C-activation to produce a single-stranded peptide **19a** in a total yield of 40%.

The ^{13}C signals of 1,12-dodecano-bis(peptide) could be assigned by ^1H–^1H 2D correlated spectroscopy (COSY), ^{13}C–^1H COSY, and distortionless enhancement by polarization transfer (DEPT) technique, and by comparison with the spectra of the constituent amino acids. The structural assignments of 1,2-ethano-bis(L-Phe–L-Phe–L-Leu) **16a** (a) and 1,12-dodecano-bis(L-Leu–L-Leu–L-Phe) **10f** (b) were made on the basis of chemical shifts and C–H COSY spectra measured by 500 MHz NMR in a 5 mM solution. The corresponding chemical shifts of the Phe^2 β- and Phe^3 β-protons (βHs) of **10f** and **16a** appeared at 2.72 and 3.08 ppm, at 2.78 and 2.98 ppm, respectively. The individual shifting of Phe^2 βH and Phe^3 βH suggests that the structure of the aromatic side chain has a rigid conformation in the intra-molecule. The ^{13}C signal of the α carbons of the key compounds, **6a** and **8a**, appeared at 56.48 ppm, and at 54.33 and 56.27 ppm, respectively. Further, the ^{13}C signals of the α carbons of **10a** were observed at 53.43, 54.13, and 54.25 ppm at higher field than the signal of **6a** and **8a**. The two $C^{\alpha}H$ signals of 1,12-dodecano-bis(D-Phe–L-Phe) **8e** were observed at 53.85 and 56.20 ppm, while the signals of the diastereomer **8f** appeared at 54.37 and 54.58 ppm in $CDCl_3$/DMSO-d_6 (0.5/0.2 v/v%). The NMR data clearly show that the double-stranded peptides have different ensemble average conformations.

CD Spectrum Studies The secondary structure of 1,2-ethano-bis(L-Phe–L-Phe–L-X) (X=Leu, Val, and without), 1,12-doecano-bis(L-Phe–L-Phe–L-X) (X=Leu, Ile, Val, and without), and 1,12-dodecano-bis(L-Phe–L-Val–L-Leu), *etc.* were examined by CD spectrometry under the same conditions in 85% methanol solution. The spectra showed the profile of the two CD spectrum types, class I and II. At CD profile of class I, the negative first Cotton effect in **10a**—**c** was observed at 237 nm, and the positive second Cotton effect which showed a large value of molar ellipticity ([θ]= 1×10^{-4} deg cm^2 dmol^{-1}), was measured at 205 nm, indicating a β-sheet or type II turn structure.[10] The CD spectra observed for the two enantiomers, **6a** and **6c**, **8a** and **8c** show the mirror image, and they are stereochemically pure. 1,12-Dodecano-bis(L-Phe–L-Phe–L-Leu) **10a** and **10h** are enantiomers. In fact, these CD spectra show the mirror image, as shown in Fig. 1.

The CD profiles of the 1,2-ethano-bis(L-Phe–L-Phe–L-Leu) **16a** and 1,12-dodecano-bis(L-Phe–L-Phe–L-Leu) **10a** are very similar to a β-sheet or type II turn-like conformation of literature data.[11] Moreover, the CD profiles of **10b**, **c**, **10h**, and **16a** (class I) were also consistent with a β-sheet mimic conformation. However, the CD profile of 1,12-dodecano-bis(L-Phe–L-Val–L-Leu) **10d** when a –L-Phe is replaced with a –L-Val is different from that of **10a**, and adopts a random conformation. In addition, the replacement of the tripeptide residue –L-Phe–L-Phe–L-Leu with –L-Leu–L-Leu–L-Phe affords **10f** and exhibits a random conformation, as shown in Fig. 2. This finding suggests that the aromatic interaction be-

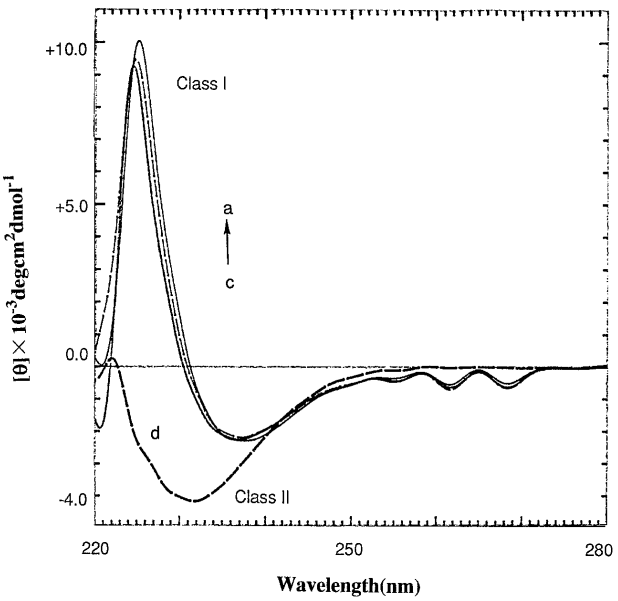

Fig. 2. Profile of CD Spectra for 1,12-Dodecano-bis(peptide)s, **10a**—**c** (a—c) and **10f** (d)

1,12-Dodecano-bis(peptide) concentration, **10a** (3.94×10^{-4} M), **10b** (5.86×10^{-4} M), **10c** (3.62×10^{-4} M), and **10f** (8.06×10^{-4} M) in 85% methanol solution at 22 °C, *x*-axis, nm; *y*-axis, molar ellipticity [θ].

tween the C-terminal Phe on both strands is a primary factor to form β-sheet-like nucleation. The relationship between conformation and sequence of amino acid residues of double-stranded peptides **2** and **3** is summarized in Table 1. Accordingly, the X–L-Phe–L-Phe–spacer(Y)–L-Phe–L-Phe–X (X=amino acids and Y=1,2-ethano- and 1,12-dodecano-, *etc*) is an important domain of mimetic mediator for β-sheet nucleation.

The depth at 237 nm of CD spectra of double-stranded peptides **6a**, **8a**, and **10a**—**c** increases in order of –L-Phe<–L-Phe–L-Phe<–L-Phe–L-Phe–L-Ile≪–L-Phe–L-Phe–L-Val<–L-Phe–L-Phe–L-Leu (Fig. 2). This order of the depth is equal to the order of mediation of β-sheet mimetic nucleation. Especially, sequences such as –L-Phe–X and –L-Phe–L-Phe–X favor a β-sheet mimic nucleation in double-stranded peptides. To further investigate the β-sheet mimic nucleation, the CD spectra of 1,2-ethano-bis(L-Phe–L-Phe–L-Leu) were measured, as shown in Fig. 3. As the CD profile of 1,2-ethano-bis(L-Phe–L-Phe–L-Leu) is similar to the profile of 1,12-dodecano-bis(L-Phe–L-Phe–L-Leu), the structure also adopts β-sheet mimic conformation. The depth at 238 nm of CD spectra of 1,2-ethano-bis(peptide)s **12a**, **14a**, and **16a** also increases in order of L-Phe–L-Phe–L-Leu≪L-Phe<L-Phe–L-Phe. The –Phe–L-Phe–L-CONHCH$_2$CH$_2$NHCO–L-

Table 1. Relationship between Types of CD Spectrum Profiles and Amino Acid Sequences of Synthesized 1,12-Dodecano-bis (A–B–C)

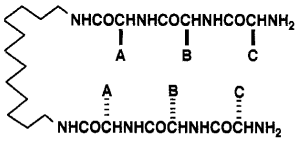

Class I[a] compound	Amino acid residue			Class II[a] compound	Amino acid residue		
	A	B	C		A	B	C
8a	Phe	Phe	—	**8b**	Ile	Ile	—
8c	Phe	Val	—	**8d**	Ile	Phe	—
10a	Phe	Phe	Leu	**10d**	Phe	Val	Leu
10b	Phe	Phe	Val	**10e**	Ile	Phe	Leu
10c	Phe	Phe	Ile	**10f**	Leu	Leu	Phe
19a[b]	Phe	Phe	Leu	**10g**	Leu	Phe	Phe

a) Type of CD spectrum profile. *b*) Single-stranded tripeptide.

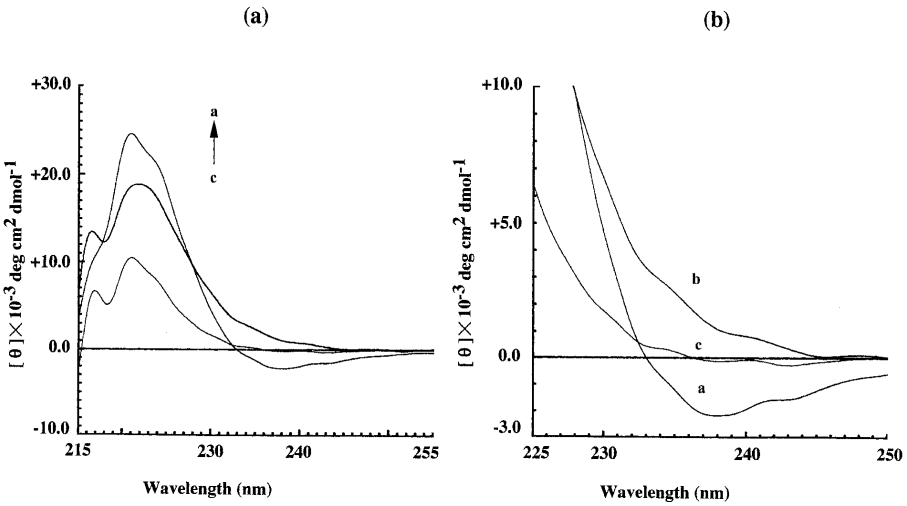

Fig. 3. Profile of CD Spectra for 1,2-Ethano-bis(peptide)s, **12a**, **14a**, and **16a**

1,2-Ethano-bis(peptide) concentration, **12a** (3.94×10^{-4} M) (c), **14a** (5.86×10^{-4} M), and **16a** (8.06×10^{-4} M) in 85% methanol solution at 22 °C, *x*-axis, nm; *y*-axis, molar ellipticity [θ].

Phe–L-Phe– domain also adopts a β-sheet or type II β-turn mimic nucleation. From these results, the sequences of –Phe–Phe–X (X=Leu, Ile, Val, *etc.*) are a useful probe for the design of β-sheet mimetic nucleation of double-stranded peptides. Thus we clarified the relationship between the conformation and amino acid residues in a double-stranded peptide. The X–L-Phe–L-Phe–spacer(Y)–L-Phe–L-Phe–X (X=Val, Ile, Leu, *etc.*; Y=1,2-ethano-, 1,12-dodecano-) forms a stable conformation for the hydrophobic interaction and intramolecular hydrogen bonding in both strands.

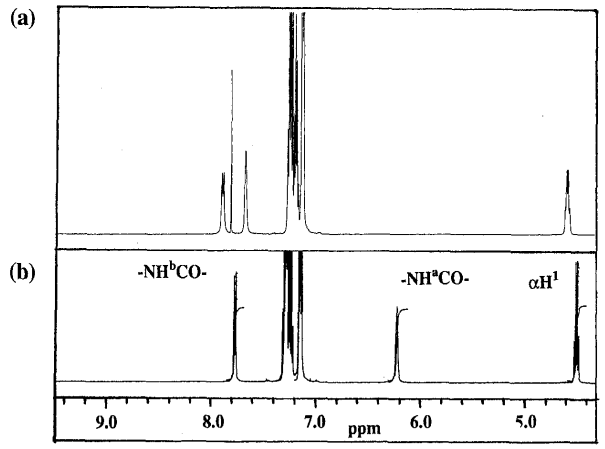

Fig. 4. Downfield Shifts of Amide, –NHCO–, Protons Chemical Shifts for 1,2-Ethano-bis(L-Phe–L-Phe) **14a** Obtained from 500 MHz Spectra in DMSO-d_6/$CDCl_3$ (Volume Ratio=0.2/0.5) (a) and in $CDCl_3$ (b)

^{1}H-NMR of Double-Stranded Peptides In $CDCl_3$/DMSO-d_6 (0.7/0.0 v/v%) (295 K) in the ^{1}H-NMR, the chemical shifts of amido –NH^a– and amido –NH^b– of 1,2-ethano-bis(L-Phe–L-Phe) **14a** appear at 6.23 and 7.77 ppm. From a ratio-dependent change of solution in the changed ratio range from $CDCl_3$/DMSO-d_6 (0.7/0.0 v/v%) to $CDCl_3$/DMSO-d_6 (0.5/0.2 v/v%), these resonances shifted to 7.68 and 7.89 ppm, respectively, as shown in Fig. 4. The difference (δ ppm) of chemical shifts of the amide protons and α protons (αH) is summarized in Table 2. The large downfield shifting ($\delta=-1.45$ ppm) of the amide proton, –NH^a–, in **14a** indicates that the amide proton favors a hydrogen-bond structure in DMSO-d_6, but the amide proton favors no hydrogen-bond structure in $CDCl_3$. In contrast, the chemical shift of the amide proton, –NH^b–, indicates that a hydrogen-bond is formed in both $CDCl_3$ and DMSO-d_6. The downfield shifting of these amide protons of **8a** and **16a** also indicates that the compounds favor the conformation of the β-sheet mimetics.[12] An interesting observation in Table 2 is that the downfield shift (−0.20 ppm) for amide proton –NH^bCO– of the diastereomer **8e** of **8a** decreases by the addition of DMSO-d_6 in $CDCl_3$ (0.5/0.2 v/v%). This indicates that the amide proton –NH^bCO– of **8e** strongly forms hydrogen bonding in $CDCl_3$.

The three amide protons, –$NH^{a,b,and\,c}$– in **16a** were observed at δ 7.67, 7.94, and 8.03 in $CDCl_3$/DMSO-d_6 solution (0.5/0.5 v/v%), respectively, and the large downfield shift of

Table 2. Solvent Shifts of Amide Protons, α-Protons, and β-Protons for Double-Stranded Peptides **8a**, **8e**, **8f**, **14a**, and **14b** in Solution

	Solvent	–NH^aCO– δ (ppm)	–NH^bCO– δ (ppm)	Phe^1 C^αH δ (ppm)	Phe^2 C^αH δ (ppm)	Phe^2 C^βH δ (ppm)
8a	$CDCl_3$	6.21	7.88	4.62	3.55	2.56
	$CDCl_3$/DMSO-d_6 [a]	7.61	8.90	4.50	4.09	2.94
	Δ ppm	−1.40	−1.02	−0.12	−0.54	−0.38
8e	$CDCl_3$	5.88	7.75	4.54	3.54	2.66
	$CDCl_3$/DMSO-d_6 [a]	7.45	7.95	4.61	3.49	2.58
	Δ ppm	−1.57	−0.20	−0.07	+0.05	+0.06
8f	$CDCl_3$ [b]	7.20	8.16	4.57	3.96	2.78
	$CDCl_3$/DMSO-d_6 [a]	7.78	8.73	4.59	4.05	2.72
	Δ ppm	−0.58	−0.57	−0.02	−0.09	+0.06
14a	$CDCl_3$	6.23	7.77	4.50	3.61	2.44
	$CDCl_3$/DMSO-d_6 [a]	7.68	7.89	4.58	3.52	2.42
	Δ ppm	−1.45	−0.12	−0.08	+0.09	+0.02
14b	$CDCl_3$	6.22	7.72	4.46	3.52	2.66
	$CDCl_3$/DMSO-d_6 [a]	7.80	8.79	4.53	3.94	2.67
	Δ ppm	−1.58	−1.07	−0.07	−0.42	−0.01

a) Conditions: $CDCl_3$/DMSO-d_6=0.5/0.2. *b*) In the presence of 2.0% DMSO-d_6.

Table 3. Solvent Shifts of Amide Protons and α-Protons for Double-Stranded Peptides **10a**, **10g**, and **16a** in Solution

		–NH^aCO– δ (ppm)	–NH^bCO– δ (ppm)	–NH^cCO– δ (ppm)	AA^1 C^αH δ (ppm)	AA^2 C^αH δ (ppm)	AA^3 C^αH δ (ppm)
10a	$CDCl_3$	6.08	6.59	7.82	4.58	4.58	4.58
	$CDCl_3$/DMSO-d_6 [a]	7.23	7.71	7.89	4.57	4.57	4.57
	Δ ppm	−1.15	−1.12	−0.07	+0.01	+0.01	+0.01
10g	$CDCl_3$ [b]	7.15	7.76	8.68	4.36	4.66	4.07
	$CDCl_3$/DMSO-d_6 [a]	7.38	8.07	8.86	4.44	4.71	4.17
	Δ ppm	−0.23	−0.31	−0.18	−0.08	−0.05	−0.10
16a	$CDCl_3$/DMSO-d_6 [c]	7.67	7.94	8.03	4.47	4.58	3.17
	DMSO-d_6	7.93	8.06	8.25	4.43	4.54	3.18
	Δ ppm	−0.26	−0.12	−0.22	+0.04	+0.04	−0.01

a) Conditions: $CDCl_3$/DMSO-d_6=0.5/0.2. *b*) In the presence of DMSO-d_6 (3.8 %). *c*) Conditions: $CDCl_3$/DMSO-d_6=0.5/0.5.

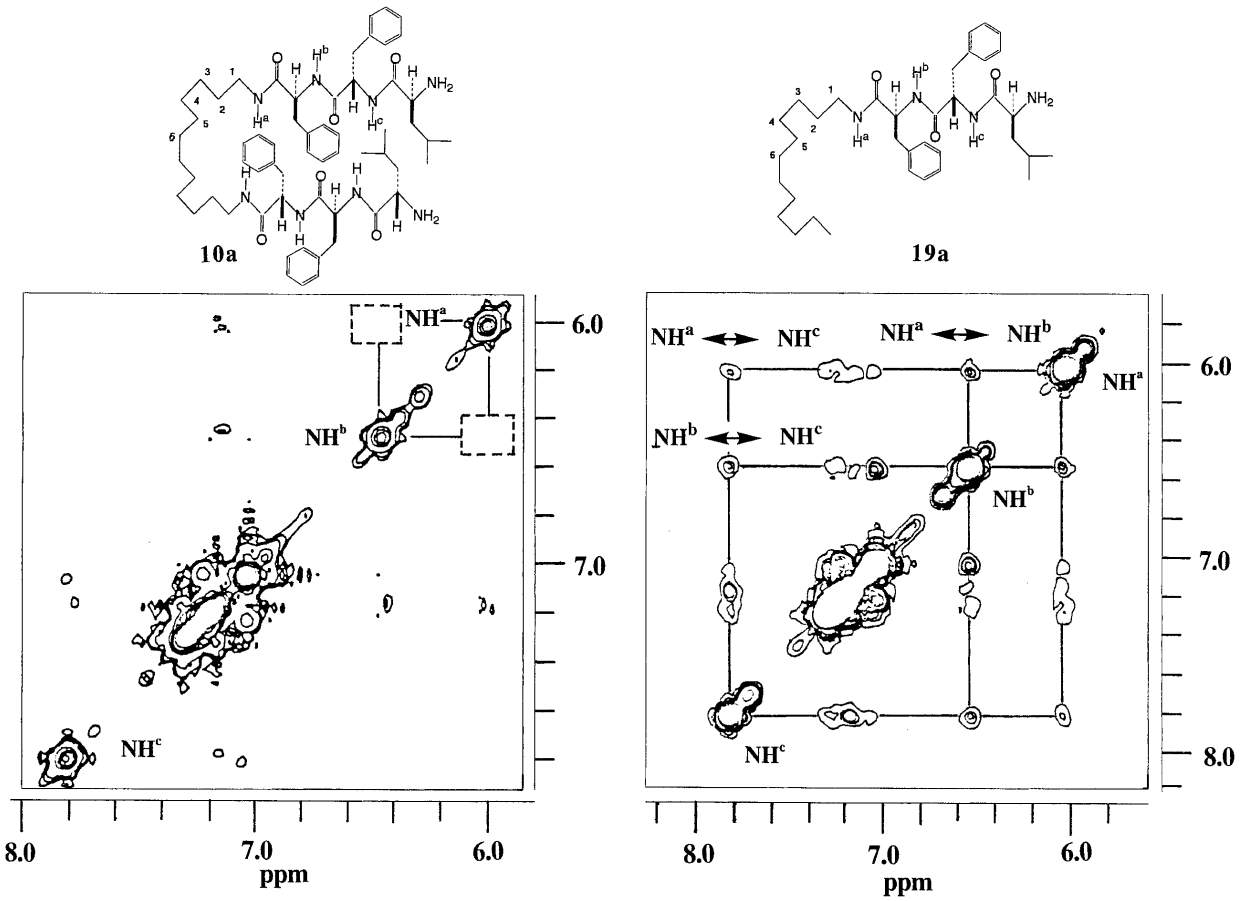

Fig. 5. NOE Cross Peaks in Amide NH Region of 500 MHz NOESY Spectra of Double-Stranded Peptide **10a** (Left) in $CDCl_3$ and Single-Stranded Peptide **19a** (Right) in $CDCl_3$

Empty boxes show absent NH^a–NH^b NOE cross peaks. Conditions: 22 °C, 6.8 mM, and 500 msec mixing time.

amide proton, –NH^aCO–, as summarized in Table 3, indicates the formation of a hydrogen bond between the amide protons of both strands. Such downfield shift of the amide proton, –NH^aCO–, also was observed in 1,12-dodecano-bis(L-Phe–L-Phe–L-Leu) **10a** and 1,12-dodecano-bis(L-Phe–L-Phe–L-Val) **10b**, and these observations support that **10a** and **10b** are an important probe for formation of a double-stranded β-turn structure.

The assignments of the NOE cross coupling between the backbone –NHCO– and $C^{\alpha}H$ of **8a**, **10a**, **10f**, **14a**, **16a**, **18a**, and **19a**, *etc.* were achieved by using 500 MHz NOESY (and/or rotating frame nuclear Overhauser and exchange spectroscopy (ROESY)) technique at a mixing time of 500 msec in $CDCl_3$ or $CDCl_3$/DMDO-d_6 (0.5/0.2 or 0.5/0.5 v/v%) solutions. The 1,12-dodecano-bis(L-Phe–L-Phe–L-LeuH) **10a** adopts the β-sheet mimic nucleation in solution, because no NOE cross peaks were observed between the three amides –$NH^{a,b,c}CO$– and $C^{\alpha}Hs$, as shown in Fig. 5 (left). The coupling constants of $^3J_{NHi,C\alpha Hi}$=8.4 Hz of Phe^1 (and $Phe^{1'}$) and $^3J_{NHi+1,C\alpha Hi+1}$=7.4 Hz of Phe^2 (and $Phe^{2'}$) also support that the conformation of **10a** adopts the nucleation mediated β-sheet mimetics in $CDCl_3$. In contrast, in the NOE cross peaks of 1,12-dodecano-bis(L-Leu–L-Leu–L-Phe) **10f**, the lack of observed NOE cross peaks between the three amide protons (–$NH^{a,b,and\,c}CO$–) and the three $C^{\alpha}H^{1,2,and\,3}$ at $C^{\alpha 1,2,and\,3}$ (α carbons$^{1,2,and\,3}$) supports that **10f** is a random conformation. Moreover, the large $^3J_{NHc,C\alpha H2}$=9.3 Hz and $^3J_{NHb,C\alpha H1}$=8.4 Hz coupling constants are also acceptable values for a random structure.[13] This observation is consistent with the result from the CD studies.

On the other hand, the $d_{\alpha N}$ NOE cross peaks between $\alpha H^1 \leftrightarrow$–$NH^aCO$–, –$\alpha H^1 \leftrightarrow$–$NH^bCO$–, and $\alpha H^2 \leftrightarrow$–$NH^bCO$– in **19a** were observed and the d_{NN} NOE strong cross peaks of –NH^aCO–$\leftrightarrow$–NH^bCO– also were observed as shown in Fig. 5 (right). This data suggests that the structure of **19a** is α-helix or 3_{10} helix[14] mimic nucleation. As the double-stranded peptide **10a** and **19a** have the same sequence residue, –L-Phe–L-Phe–L-Leu (N terminus), the pattern of NOE cross peaks should be similar; however, the pattern of NOE cross peaks is dissimilar (left in Fig. 5). The NOE data clearly support that the double-stranded peptide **10a** has a very different time average conformation from the single-stranded peptide **19a**. The strong d_{NN} connectivities show that the peptide chains of **19a** mediate α-helical mimic nucleation. Therefore, the reason why **10a** is different from the conformation in spite of the same sequence is derived from the parallel double-strand effect by the dodecano spacer. This behavior of NOE cross peaks of **10a** is most likely a result of the interaction of the one strand with the other strand in the double-stranded peptides. As expected, the structures of double-stranded peptides are influenced by an intramolecular interaction between the two strands.

The NOE cross peaks are present in between Phe^1 aH and *o*-protons of Phe^2 side chain on 1,12-dodecano-bis(L-Phe–D-Phe) **8f**. The observation of NOE cross peaks between dodecano-spacer protons and aromatic protons of Phe in **8a** and

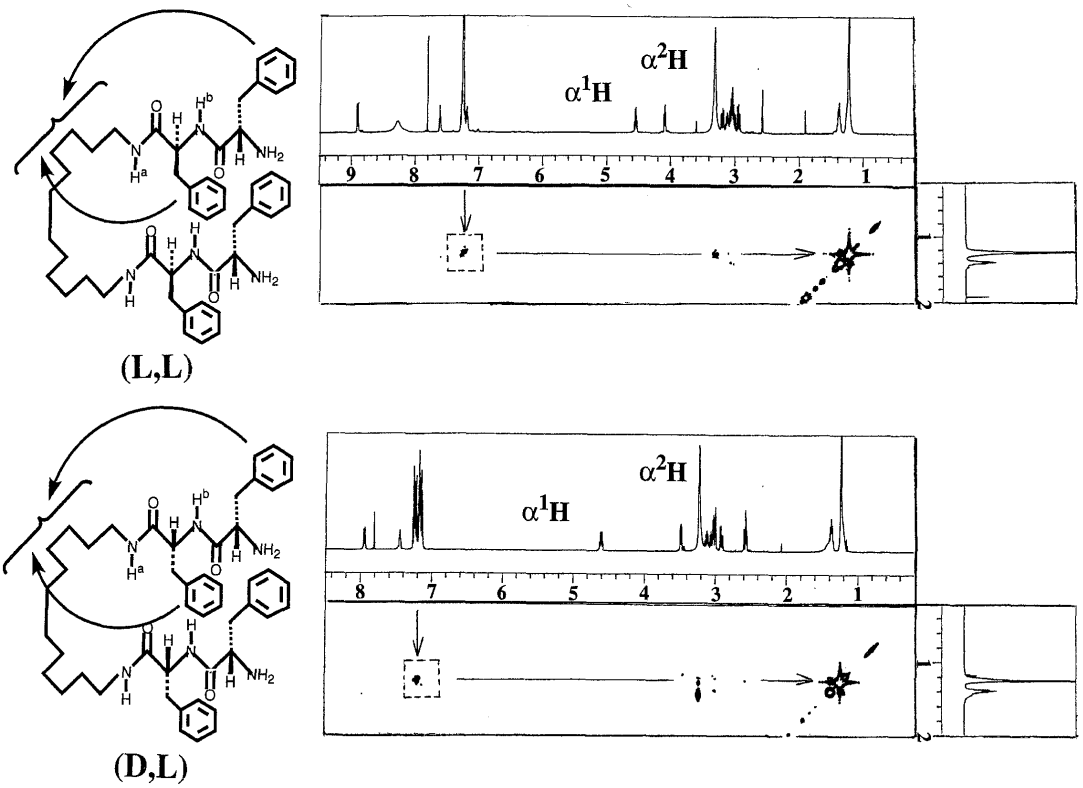

Fig. 6. NOE Cross Peaks in Aromatic Protons–Spacer Protons Region of 500 MHz NOESY Spectra of Double-Stranded Peptides **8a** (a) and **8e** (b)
Boxes show aromatic protons–spacer protons NOE cross peaks. Conditions: 22 °C, 10.0 mM, and 500 msec mixing time.

8e confirms the folded structure, as shown in Fig. 6, because the cross peaks suggest that the conformation adopts a more β-turn-like-structure than the linear structure. As an interesting long-range NOE cross peak is also observed between Phe[1] aH and amido proton –NH^{a}CO– in 1,2-ethano-bis(L-Phe–L-Phe–L-Leu) **16a**, it suggests that **16a** is a folded conformation. Similar NOE cross peaks in the NOESY spectra also could be obtained in **10a**, **10b**, **10g**, **16a**, and **16b**, *etc.* so that the distance between the protons of spacer and the aromatic protons of Phe side chain (and protons of Me groups in Leu) is within 3.5 Å for double-stranded peptides in DMSO-d_6/$CDCl_3$ solution. In addition, the low $J_{NHa,C1H2}$ coupling constants (=5.2—5.5 Hz) with the spacer's proton (–C^{1}H$_2$–) of the amido proton, –NH^{a}CO–, also support a β-turn-like-conformation at –C^{2}H$_2$–C^{1}H$_2$–NH–CO– (dihedral angle; $\omega=-70°$) of each strand folded structure for **8a**, **8e**, **10b**, and **10f**, *etc.* In the NMR of **10a** in $CDCl_3$, the selective upfield shifts of *o*-hydrogen (δ=7.02 ppm) of the Phe side chain are originate from a strong interaction such as anisotropy effect and suggest that the *o*-hydrogen interacts with the other Phe with edge-to-face geometry.

Conformations, Dihedral Angle (θ), and Energy Calculations The energy calculations were performed by use of the MM2 method[7] to obtain the low-energy conformational geometry of the mini parallel double-stranded peptides. For conformers of 1,2-ethano-bis(L-Phe–L-Phe) **14a** and 1,12-dodecano-bis(L-Phe–L-Phe) **8a**, four dihedral angles ϕ (CO–NH–C$^\alpha$H–CO), ψ (NH–C$^\alpha$H–CO–NH), ω (CO–NH–CH_2–CH_2), and θ ($\angle$NH^a–C^1–C^2–NH^a or $\angle$C^5–C^6–C^7–C^8) were considered, and the calculations were performed with under constraints for the dihedral angles, θ (from 0 to 180°—195° rotation) and ψ. The J values measured by NMR were translated to the dihedral angles, ϕ and ω, by using the Karplus equation[15,16] and the resulting data are summarized in Tables 4 and 5. The low-energy conformers of **8a** and **14a** match the conformation proposed from experimental results (NOEs, $J_{NH,\alpha H}$ and $J_{C1,NH}$) so that the β-turn-like-conformer is better than the linear conformer.

The average dihedral angles, ϕ and ω, of **14a** were determined from coupling constants, $J_{NHb,\alpha H1}$=7.6 Hz and $J_{NHa,C1H2}$=4.4 Hz (**16a**) in $CDCl_3$/DMSO-d_6 solution. Compound **14a** has average dihedral angles of $\phi=-87°$ and $\omega=+90°$.[17] The dihedral angles ($\omega=-90°$, $\phi=-87°$, $\psi=+180°$) indicate a β-turn-like structure. The minimized steric energy of **14a** is −28.4 kcal/mol at $\theta=-15°$, and the steric energy at $\theta=+180°$ is −21.6 kcal/mol, and the most probable conformers ($\omega=+90°$, $\phi=-87°$, $\psi=+180°$, $\theta=-15°$, form *a*) of **14a** are presented in Fig. 7. The steric energy for the β-turn-like structure is lower than that of α-helical mimic structure at dihedral angles ($\omega=+90°$, $\phi=-47°$, $\psi=-57°$) in $CDCl_3$/DMSO-d_6 solution. The dihedral angle ($\omega=+90°$) of 1,2-ethano-bis(D-Leu) observed by ^{1}H-NMR almost coincided with the value ($\omega=+95°$) obtained by X-ray crystallography.[17] These findings support that **14a** favors a β-turn-like structure.

The dihedral angles, ϕ and ω, of **8a** were determined from coupling constants, $J_{NHb,\alpha H1}$=7.6 Hz and $J_{NHa,C1H2}$=5.4 Hz. The geometries of the conformer were minimized under constraints for backbone dihedral angles, $\phi=-89°$, $\psi=+180°$, $\omega=-70°$ obtained by the experiments. Under the constraint, particularly, we calculated the low-energy conformers of **8a** varied for dihedral angle, θ, from 0 to 210°, as plots of θ dependence energy in Fig. 8. The low-energy conformers $\theta=+75°$ ($\Delta E=-3.8$ kcal/mol) and 180° ($\Delta E=-7.9$ kcal/mol) obtained at $\psi=+180°$ which are more stable than the conformers at $\psi=+115°$. The structure of **8a** was as-

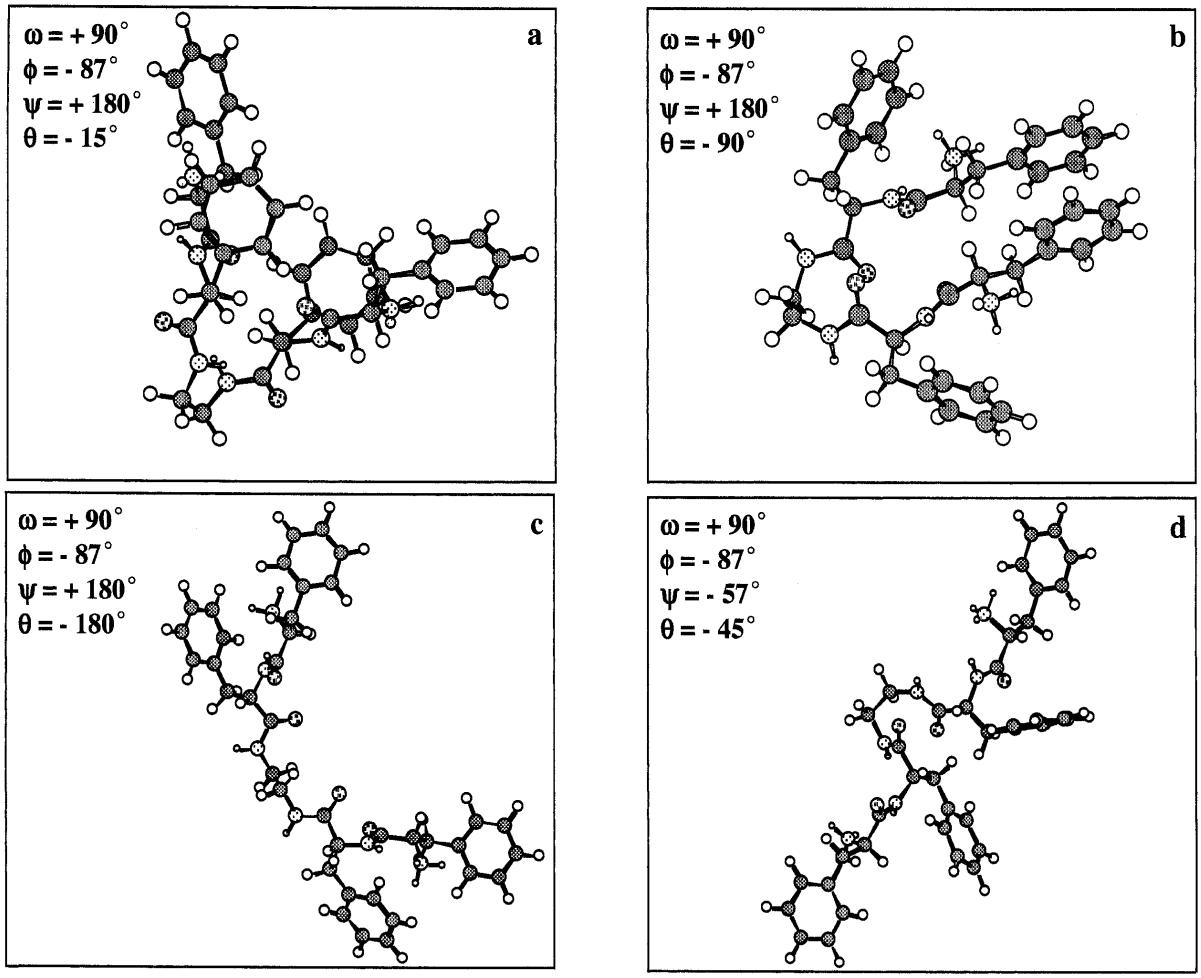

Fig. 7. Cylindrial Bonds Representation of Proposed Most Stable Conformers of 1,2-Ethano-bis(L-Phe–L-Phe) **14a**

The calculation is performed for **14a**, based on the NOE connectivities and observed coupling constant (J Hz). The conformer a is the most stable at dihedral angle $\theta=-15°$ and a—c adopt a nucleation mediate by a β-turn-like structure. The energy minimized conformer d ($\theta=-45°$) calculated under constraints for dihedral angle ($\omega=+90°$, $\phi=-47°$, and $\psi=-57°$), and adopts a α-helix-like structure.

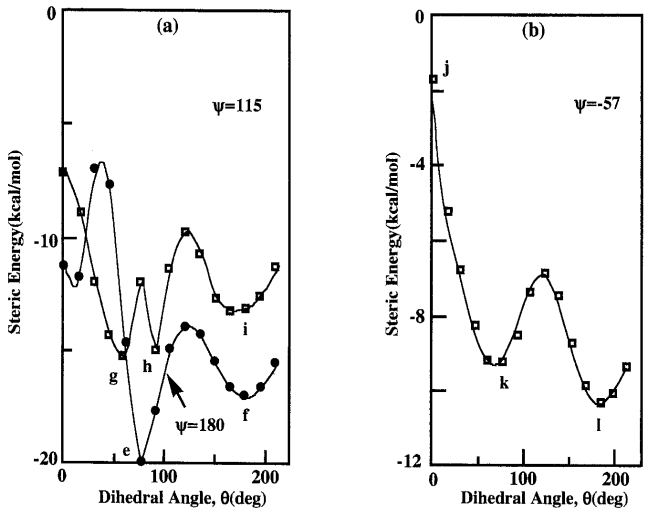

Fig. 8. Steric Energies for 1,12-Dodecano-bis(L-Phe–L-Phe) **8a** as Calculated Using MM2 as a Function of Dihedral Angle (θ)

Energy was calculated under constraint using the corresponding dihedral angles, $\omega=-70°$, $\phi=-89°$, and $\psi=+115°$ (and $\psi=+180°$) (a), and $\omega=-70°$, $\phi=-47°$, and $\psi=-57°$ (b), determined from the observed $^3J_{\alpha N}$ (Hz). The (a) and (b) introduced **8a** in a turn β-strand and a turn α-strand conformation, respectively.

signed to a spiral β-turn-like structure ($\phi=-89°$, $\psi=+180°$, $\theta=+75°$ or 180°). The results are satisfied with the Ramachandran angles. The most probable conformers ($\omega=-70°$, $\phi=-89°$, $\psi=+180°$, $\theta=+75°$, form e) of **8a** are presented in Fig. 9. Here, if **8a** is a structure mediated α-helical mimic nucleation, the compound has average dihedral angles of $\phi=-47°$ and $\psi=-57°$. Figure 9b shows the plot of θ dependence of energy. If **8a** is a nucleation mediated α-helical mimic structure, the low-energy conformers are energically more unstable than that of the β-turn structure. The coupling constant ($J_{\mathrm{NHb},\alpha\mathrm{H1}}$) should provide *ca.* 3.9 Hz.[18] In summary, the structure of parallel double-stranded peptides **8a** and **10a** (not shown here), *etc.* nucleates a parallel β-turn-like conformation and two low-energy conformers are generated under constraints at dihedral angles $\phi=-89°$ and $\psi=+180°$ rotation (Fig. 9).

Binding Affinity In order to investigate the chemical properties of double-stranded peptides, which form a β-turn-like conformation, binding studies were performed by UV-visible optical titration under Baba–Nagakura type conditions ($[L_0]<[H_i]$) to determine the association constants K_a (M^{-1}).[19] The method of titration is provided in the experimental section.

$$[H_i][H_j]\times(A_j-A_i)\times K_a=[H_i]\times(A_0-A_i)\times[H_j]\times(A_i-A_0) \quad (1)$$

Table 4. Minimum Energy and Corresponding Dihedral Angles (θ, ω, ψ, ϕ) of **14a** Determined from Experimental Coupling Constants Values (J) and Calculations

Compounds[a]	$-CH_2-CH_2-NH-CO-$ ω	$-NH-CO-CH-NH-$ ψ_1	$-CO-CH-NH-CO-$ ϕ_1	$-NH-CO-CH-NH-$ ψ_2	$-CH_2-CH_2-CH_2-CH_2-$ θ	Steric energy (kcal/mol)
Turn β-sheet mimetics						
14a a	+90	+180	−87	+31.5[b]	−15	−28.40
b	+90	+180	−87	+44.2[b]	−90	−23.16
c	+90	+180	−87	+36.6[b]	−180	−21.58
Turn α-helical mimetics						
14a d	+90	−57	−87	−47	−45	−27.19

a) See Fig. 7 for description of backbone dihedral angles (θ) and structures of the double-stranded peptides. *b*) Calculated values.

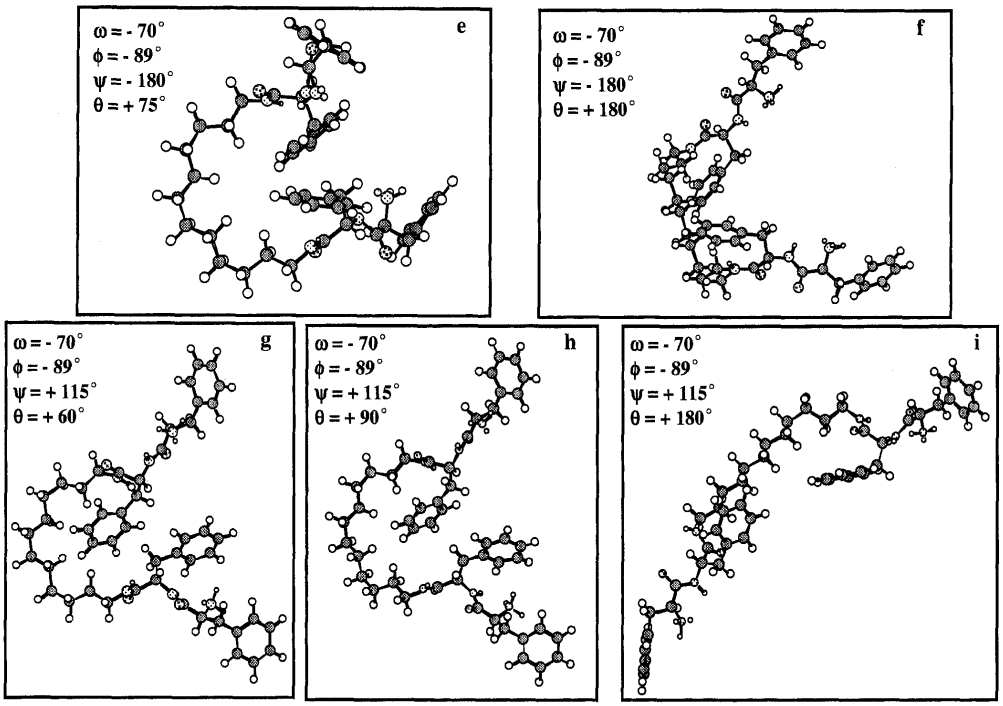

Fig. 9. Cylindrial Bonds Representation of Proposed Most Stable Conformers of 1,12-Dodecano-bis(L-Phe–L-Phe) **8a**

The calculation is performed for **8a**, based on the NOE connectivities and observed coupling constants (J Hz). From Fig. 8a, the e and f are the most probable conformations (θ=+75° and +180°) and adopt a β-turn-like structure. The ψ=+115° of conformers g, h, and i is chosen to reflect typical dihedral angle ψ for β-sheet structure to compare e and f with g, h, and i conformers.

Table 5. Minimum Energy and Corresponding Dihedral Angles (θ, ω, ψ, ϕ) of **8a** Determined from Experimental Coupling Constants Values (J) and Calculations

Compounds[a]	$-CH_2-CH_2-NH-CO-$ ω	$-NH-CO-CH-NH-$ ψ_1	$-CO-CH-NH-CO-$ ϕ_1	$-NH-CO-CH-NH-$ ψ_2	$-CH_2-CH_2-CH_2-CH_2-$ θ	Steric energy (kcal/mol)
Turn β-sheet mimetics						
8a e	−70	−180	−89	+24.4/+43.8[b]	+75	−19.94
f	−70	−180	−89	+27.4/+45.6[b]	+180	−17.00
g	−70	+115	−89	+31.1/+34.8[b]	+60	−15.19
h	−70	+115	−89	+31/+34.8[b]	+90	−15.00
i	−70	+115	−89	++31.2/+44.9[b]	+180	−13.16
Turn α-helical mimetics						
8a j	−70	−57	−47	−47	+0	−1.72
k	−70	−57	−47	−47	+75	−9.22
l	−70	−57	−47	−47	+180	−10.32

a) See Figs. 8 and 9 for description of backbone dihedral angles (θ) and structures of the double-stranded peptides. *b*) Calculated values.

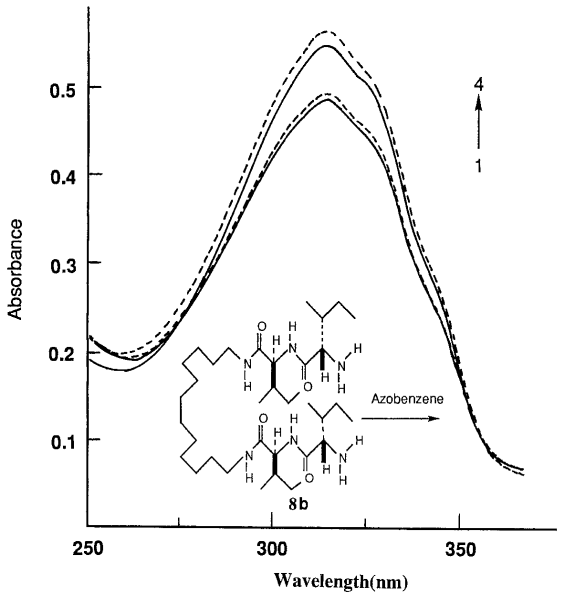

Fig. 10. Electronic Absorption Titration to Determine the Association Constant of Complex between **8b** and Azobenzene in Methanol at T=295 K

In titration, $[L_0]$ is 2.11×10^{-5} M, and $[H_i]$ are the following from spectrum 1 to spectrum 4: 0.00, 0.998, 9.89, and 59.9×10^{-5} M.

Table 6. Association Constants K_a (M^{-1}) and Free Energy of Formation ΔG of 1,12-Dodecano-bis(peptide)–Guest Molecular Complex in Methanol Solution

Compound	CD type	Guest	K_a ($\times10^4$)	$-\Delta G$ (kcal/mol)	T(K)
8a	Class I	Azobenzene	0.96	5.4	298
8b	Class II	Azobenzene	1.2	5.5	295
8a	Class I	Pyrene	3.5	6.2	298
8b	Class II	Pyrene	0.29	4.7	298
10a	Class I	Azobenzene	1.0	5.5	297
10b	Class I	Azobenzene	0.81	5.3	295
10c	Class II	Azobenzene	0.028	3.3	295
10a	Class I	PHA	0.13	4.2	296
10d	Class II	PHA	0.048	3.6	296

$$-\Delta G=\boldsymbol{R}\mathrm{T}\times\ln K_a \quad (2)$$

In Eq. 1, A_0, A_i, and A_j are the absorbance of the guest (substrate) when molar concentration of the host (dodecano double strand peptide) is $[L_0]$, $[H_i]$, and $[H_j]$, respectively. The values of a free energy of formation, $-\Delta G$ (kcal/mol), of the host–guest complex were calculated by Eq. 2. The guests, azobenzene, pyrene, or *N*-phenyl-1-naphthylamine (PHA) were used in all cases to determine K_a, since there is non-overlapping absorption with that of Phe.

As seen in a typical titration curve of Fig. 10, the titration spectrum with 1,12-dodecano-bis(L-Ile–L-Ile) **8b** and azobenzene (guest, $[L_0]=2.11\times10^{-5}\,M^{-1}$) was consistent with formation of a 1 : 1 inclusion complex with an isosbestic point at about 280 and 360 nm. The K_a was estimated to be 1.2×10^4 (M^{-1}) $[=(1.22+1.24+1.03)/3\times10^4]$ as the mean value of the apparent K_i obtained from the absorbance (A_i) at 310, 320, and 330 nm in methanol. The $-\Delta G$ of **8a** pyrene complex (=6.2 kcal/mol) is 1.5 kcal/mol larger than that of **8b**·pyrene complex (=4.7 kcal/mol). The increase in its binding energy means that the hydrophobicity of the binding site in dodecano double-stranded peptides is increased by the side chain on the Phe residue. When the replacement of a single residue (from Phe to Ile) in **10a** is afforded, the intensity of the binding constant is higher than that of **10e**. In fact, the stability of inclusion complex formation increased in order of **10a**·azobenzene>**10b**·azobenzene>**10d**·azobenzene. The thermodynamic data for the binding complex are summarized in Table 6. For understanding structure–function relationship based on the order, we studied the binding with the double-strand peptides of PHA. A similar result, for instance, was obtained from the complex formation by interaction with **10a** and **10d** of PHA. The results showed that the stability increases in order of **10a**·PHA>**10d**·PHA. We examined how the substrates fit into the size and conformation of the binding site. Table 7 shows that the diastereoselectivity of 1,2-ethano-bis(L-Phe–L-Phe) **14a** and 1,2-ethano-bis(L-Phe–D-Phe) **14b** for substrate (azobenzene) was observed, and $-\Delta G$ energy for inclusion complex, 1,2-ethano-bis(L-Phe–D-Phe)·azobenzene, increases about 0.5 kcal/mol compared with 1,2-ethano-bis(L-Phe–L-Phe)·azobenzene complex.

Table 7. Association Constants K_a (M^{-1}) and Free Energy of Formation ΔG of 1,2-Ethano-bis(peptide)–Guest Molecular Complex in Methanol Solution

Compound	CD type	Guest	K_a ($\times10^4$)	$-\Delta G$ (kcal/mol)	T(K)
14a	—	Azobenzene	0.348	4.8	297
14b	—	Azobenzene	0.83	5.3	297
16a	Class I	Azobenzene	0.165	4.3	297

By including the substrate in the binding site, the peptide mimetic system gave binding constants that are different by several kilocalories by changing the amino acid of the host, as shown in Table 6. The intensity change in the binding energy indicates that the binding site of class I type in double strand peptides is strongly lipophilic, compared to the class II type. According to the hydrophobic parameter value (π) of several amino acids reported by Akamatsu and Fujita[11c] replacement of a single residue –Ile–Ile from **8b** to –Phe–Phe **8a** increases the sum of the hydrophobic parameter from 3.62 to 3.90. Consequently, the thermodynamic data demonstrate the importance of the hydrophobic parameter on the double-stranded peptides. Interestingly, the **6a**·chalcone complex with an electron withdrawing group in the intermolecule, of **6a** increases the $-\Delta G$ (=6.9 kcal/mol), depending on the effect of π–π stacking based on the charge transfer between chalcone and side chain on the residue. The best hosts (=the artificial receptors) for binding with the substrate are observed with Class I CD type of the double-stranded peptides and probably resulted from fit orientation of substrate within binding site of –L-Phe–L-Phe–L-X (X=amino acid) from NMR studies as described in the previous section. Our results show that the double-stranded peptides of class I CD type bind with substrate stronger than those of class II CD type.

Conclusion

In this work, double-stranded peptides, X^3–L-Phe^2–L-Phe^1–spacer(S)–L-Phe^1–L-Phe^2–X^3 (X=amino acids; S=ethano- and dodecano-) were designed and synthesized to clarify the chemical function of the –Phe–Phe–Val– sequence (and analogs) contained in Alzheimer's disease related β-

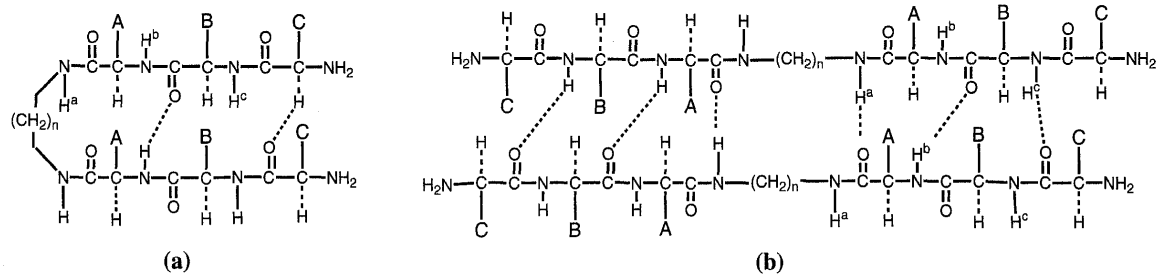

Fig. 11. Structure of Double-Stranded Peptides

(a) Intramolecular folding structure. (b) Interstranded dimer by hydrogen-bonding. Where A—C represent the corresponding amino acid residues.

amyloid peptide. The ^{1}H-NMR and CD studies indicate that the double-stranded peptides are a chemical skeleton mediated β-turn sheet mimetic structure. However, the other double-stranded peptide, Phe^3–L-Leu^2–L-Leu^1–(S)–Leu^1–L-Leu^2–L-Phe^3 (S=dodecano-), *etc.* mediates a turn random-form nucleation. The difference in the two conformations indicates that the hydrophobic interactions between Phe^1 and Phe^2 of each strand are promoted by the formation of the parallel β-turn sheet mimetics. From computational chemical (energy potential diagram) and experimental results, the results can be summarized as follows.

(i) The turn-structure and -conformation of double-stranded peptides also were confirmed by the thermodynamic data for the inclusion of substrate.

(ii) The CD profiles of X^3–L-Phe^2–L-Phe^1–spacer(S)–L-Phe^1–L-Phe^2–X^3 were consistent with literature data of a β-turn sheet mimic conformation.

(iii) The β-sheet conformation was characterized by $J_{\mathrm{NHb},\alpha\mathrm{H1}}$ value in the range from 7 to 9 Hz.

(iv) The geometry based on NOESY, $J_{\mathrm{NHb},\alpha\mathrm{H1}}$ values, and computational calculation of 1,12-dodecano-bis(L-Phe^1–L-Phe^2) has the average dihedral angles at $\omega=-70°$, $\phi=-89°$, $\psi=+115°$, $\theta=+75°$ (and $+180°$) and adopts a structure mediated parallel β-turn sheet-like conformation in solution.

(v) The selective downfield shift of the amide protons on double-stranded peptide also suggests the possibility of β-turn sheet and hydrogen bonding interaction, as shown in Fig. 11.

(vi) The presence of a low-concentration of $d_{\mathrm{NHa},\alpha\mathrm{H1}}$ and $d_{\mathrm{Phe,spacer}}$ supports an intrastranded hydrogen bonding (a) in a double-stranded peptide, but not the interstranded hydrogen bonding between dimer (b), as shown in Fig. 11.

The chemical and biological functions of –Phe–Phe–Val– or –Phe–Phe– sequences contained in Alzheimer's disease related β-amyloid peptide are not known yet, however our results support that the sequences play an important role to replace the conformation to β-sheet structure. The double-stranded peptides should prove to be very useful compounds in medicinal chemistry. Further study of these and related double-stranded peptides should continue to provide insight on the origins of turn β-sheet and biological activities.

Experimental

Materials Melting points were taken on a Yanako (MP-21) apparatus and are uncorrected. IR spectra were recorded with a JASCO A-100 spectrophotometer and UV-visible spectra with a JASCO U-best 30 spectrophotometer. ^{1}H- and ^{13}C-NMR spectra were recorded with a JNM GX-270 (270 MHz), α-500 (500 MHz), or Valian GEMINI 300 (300 MHz) spectrometer with TMS (tetramethylsilane) as an internal standard. FAB mass spectral data were recorded with a JEOL JMS-HX110 spectrometer, and relevant data are tabulated as *m/z*. TLC was performed using Silica gel 60 F_{254} (Merck) plates and the following solvent systems: $CHCl_3$–MeOH (20 : 1) (A) and $CHCl_3$–MeOH (10 : 1) (B). The peptides were detected on the TLC plates using iodine vapor or UV absorption. Silica gel column chromatography was performed on Wako gel C-200 (100 mesh) or Merck Silica gel 60N (100 mesh). Analytical RP-HPLC was carried out on a TOSO CCPD system equipped with a Tskgel (ODS-120T) column. Elemental analyses were done as by Yanako HCN corder (MT-3). All UV-vis and CD spectra used commercial solvents of the highest available purity for spectroscopy.

Typical Synthesis. Typical Synthesis of the 1,12-Dodecano-bis(L-PheZ) (5a) CDI (3.98 g, 22.0 mmol) was added to a solution of Z–L-PheOH (6.20 g, 21.0 mmol) in dry $CHCl_3$ (50 ml). After stirring for 1.5 h at room temperature, 1,12-dodecanodiamine **4** (2.0 g, 10.0 mmol) was added to the stirred solution, then stirred overnight. This solution was evaporated to dryness. After addition of aq. MeOH, the solid was collected, and washed with aq. MeOH, 5% citric acid, 5% $NaHCO_3$, and water, and dried *in vacuo*. The resulting product, **5a**, a colorless solid was obtained in 97.0% yield, and the crude product (3.5 g) was purified by column chromatography on silica gel (45 g) eluted with $CHCl_3$ and 3% MeOH/$CHCl_3$ (stepwise elution); mp 157—158 °C (from aq. MeOH); *Rf* (A): 0.59; FAB-MS *m/z* 764 (M^++1).

1,12-Dodecano-bis(L-Phe–L-Phe–L-ValBoc) (9b) To a magnetically stirred solution of 1,12-dodecano-bis(L-Phe–L-Phe) **8a** (1.65 g, 2.1 mmol), Boc–L-ValOH (0.934 g, 4.3 mmol), and triethylamine (TEA) (0.62 ml) in dry DMF (20 ml) was added DEPC (0.86 g, 5.3 mmol) at 4 °C. The resulting solution was stirred at 4 °C for 1 h and then at room temperature overnight. The solution was poured into ice/water, and the precipitate was collected by filtration, washed with 5% citric acid, 5% $NaHCO_3$, and water, and dried to give colorless crystals of **9b**: 81.0% yield, and the product was purified by column chromatography on silica gel (45.0 g) eluted with $CHCl_3$ and 3% MeOH/$CHCl_3$ (stepwise elution); mp 198—200 °C; *Rf* (A): 0.36; HR-FAB-MS (nitrobenzylalchohol) *m/z* 1188 (M^++1): Found 1187.7490, Calcd for $C_{68}H_{99}N_8O_{10}$ 1187.7485.

The following compounds, **5a**—**9h** were prepared from the corresponding Z(or Boc)-protected amino acid similarly to the above described method. 1,12-Dodecano-bis(L-IleZ) **5b**: 85.0% yield; mp 142—143 °C (from ether/MeOH); *Rf* (A) 0.24. 1,12-Dodecano-bis(D-PheBoc) **5c**: 91.0% yield; mp 125—127 °C (from ether/MeOH); *Rf* (A) 0.76; FAB-MS (nitrobenzyl alchohol) *m/z* 696 (M^++1). 1,12-Dodecano-bis(L-LeuZ) **5d**: 95.7% yield; mp 97—99 °C; *Rf* (A) 0.87; FAB-MS (nitrobenzyl alchohol) *m/z* 696 (M^++1). 1,12-Dodecano-bis(L-Phe–L-PheZ) **7a**: 96.5% yield; mp 201—202 °C (from MeOH); *Rf* (A) 0.49; FAB-MS (nitrobenzyl alchohol) *m/z* 1058 (M^++1). 1,12-Dodecano-bis(L-Ile–L-IleZ) **7b**: 89.0% yield; mp 180—183 °C (from MeOH); *Rf* (A) 0.45; FAB-MS (nitrobenzyl alchohol) *m/z* 946 (M^++1). 1,12-Dodecano-bis(L-Phe–L-ValBoc) **7c**: 98.5% yield; mp 145—147 °C; *Rf* (A) 0.55; HR-FAB-MS (nitrobenzyl alchohol) *m/z* 894 (M^++1): Found 893.6116, Calcd for $C_{50}H_{81}N_6O_8$ 893.6118. 1,12-Dodecano-bis(L-Ile–L-PheZ) **7d**: 95.6% yield; mp 205—206 °C; *Rf* (A) 0.67; FAB-MS (nitrobenzyl alchohol) *m/z* 990 (M^++1). 1,12-Dodecano-bis(D-Phe–L-PheBoc) **7e**: 83.1% yield; mp 178—180 °C; *Rf* (A) 0.76; HR-FAB-MS (nitrobenzyl alchohol) *m/z* 990 (M^++1): Found 989.6118, Calcd for $C_{58}H_{81}N_6O_8$ 989.6116. 1,12-Dodecano-bis(L-Phe–D-PheZ) **7f**: 86.7% yield; mp 182—184 °C; *Rf* (A) 0.32; HR-FAB-MS (nitrobenzyl alchohol) *m/z* 1058 (M^++1): Found 1057.5809, Calcd for $C_{64}H_{77}N_6O_8$ 1057.5803. 1,12-Dodecano-bis(D-Phe–D-PheBoc) **7g**: 83.0% yield; mp 186—187 °C; *Rf* (A) 0.47; FAB-MS (nitrobenzyl alchohol) *m/z* 990 (M^++1). 1,12-Dodecano-bis(L-Leu–L-PheZ) **7h**: 92.3% yield; mp 231—232 °C; *Rf* (A) 0.67; FAB-MS (nitrobenzyl alchohol) *m/z* 990 (M^++1). 1,12-Dodecano-bis(L-Phe–L-Phe–L-

LeuZ) **9a**: 91.8% yield; mp 206—208 °C (from ether/MeOH); *Rf* (A) 0.23; FAB-MS (nitrobenzyl alchohol) *m/z* 1284 (M^++1). 1,12-Dodecano-bis(L-Phe–L-Phe–L-IleZ) **9c**: 90% yield; mp 207—210 °C (from MeOH); *Rf* (B) 0.57. 1,12-Dodecano-bis(L-Phe–L-Val–L-LeuBoc) **9d**: 85.2% yield; mp 234—236 °C (from MeOH); *Rf* (A) 0.41; HR-FAB-MS (nitrobenzyl alchohol) *m/z* 1120 (M^++1): mass found 1119.7828, Calcd for $C_{62}H_{103}N_8O_{10}$ 1119.7800. 1,12-Dodecano-bis(L-Ile–L-Phe–L-LeuZ) **9e**: 83.0% yield; mp 195—198 °C (from MeOH); *Rf* (A) 0.48; FAB-MS (nitrobenzyl alchohol) *m/z* 1216 (M^++1). 1,12-Dodecano-bis(L-Leu–L-Leu–L-PheZ) **9f**: 87.9% yield; mp 193—195 °C (from MeOH); *Rf* (A) 0.26; FAB-MS *m/z* 1216 (M^++1). 1,12-Dodecano-bis(L-Leu–L-Phe–L-PheBoc) **9g**: 85.5% yield; mp 175—177 °C (from MeOH); *Rf* (B) 0.81; HR-FAB-MS (nitrobenzyl alchohol) *m/z* 1216 (M^++1): Found 1215.7792, Calcd for $C_{70}H_{103}N_8O_{10}$ 1215.7796. 1,12-Dodecano-bis(D-Phe–D-Phe–D-LeuZ) **9h**: 91.0% yield; mp 205—207 °C; *Rf* (A) 0.55; HR-FAB-MS (nitrobenzyl alchohol) *m/z* 1284 (M^++1): Found 1284.7579, Calcd for $C_{76}H_{100}N_8O_{10}$ 1284.7566.

Synthesis of the 1,2-Ethano-bis(L-(or D-)amino acid). 1,2-Ethano-bis(L-Phe–L-Phe–L-ValBoc) 15b To a magnetically stirred solution of 1,2-ethano-bis(L-Phe–L-Phe) **14a** (0.49 g, 0.76 mmol), Boc-L-ValOH (0.35 g, 1.6 mmol), and TEA (0.2 ml) in dry DMF (10 ml) was added DEPC (0.35 g, 2.2 mmol) at 4 °C. The resulting solution was stirred at 4 °C for 1 h and then at room temperature overnight. The solution was poured into ice/water, and then the precipitates were collected, washed with 5% citric acid, 5% $NaHCO_3$, and water, and dried *in vacuo*: 87.0% yield. The crude material obtained was purified on a silica gel (50 g) column chromatography eluting with $CHCl_3$ and 3% MeOH/$CHCl_3$ (stepwise elution) to give 1,2-ethano-bis(L-Phe–L-Phe–L-ValBoc) **15b** as a colorless crystals: mp 263—265 °C; TLC *Rf* (A) 0.38; HR-FAB-MS (nitrobenzyl alchohol) *m/z* 1048 (M^++1): Found 1047.5923, Calcd for $C_{58}H_{79}N_8O_{10}$ 1047.5919.

The following compounds, **11a**—**15a** were prepared from the corresponding Z(or Boc)-protected amino acid similarly to the above described method. 1,2-Ethano-bis(L-PheBoc) **11a**: 96.4% yield; mp 195—197 °C; *Rf* (A) 0.35. 1,2-Ethano-bis(L-LeuZ) **11b**: 95.8% yield; mp 190—192 °C; *Rf* (A) 0.40. 1,2-Ethano-bis(D-LeuZ) **11c**: 87.6% yield; mp 191—193 °C; *Rf* (A) 0.42. 1,2-Ethano-bis(L-Phe–L-PheBoc) **13a**: 97.9% yield; mp 225—227 °C; *Rf* (A) 0.33; HR-FAB-MS (nitrobenzyl alchohol) *m/z* 850 (M^++1): Found 849.4521, Calcd for $C_{48}H_{61}N_6O_8$ 849.4556. 1,2-Ethano-bis(L-Phe–D-Phe-Boc) **13b**: 95.5% yield; mp 230—232 °C; *Rf* (A) 0.25; FAB-MS (nitrobenzyl alchohol) *m/z* 850 (M^++1). 1,2-Ethano-bis(L-Phe–L-Phe–L-LeuBoc) **15a**: 73.0% yield; mp 248—250 °C; *Rf* (A) 0.48; HR-FAB-MS (nitrobenzyl alchohol) *m/z* 1076 (M^++1): Found 1075.6207, Calcd for $C_{60}H_{83}N_8O_{10}$ 1075.6230.

Synthesis of the Lauryl-L-(or D-)amino Acids The following compounds, **17b** were prepared from the corresponding Z-protected amino acid with similarly to the above described method. Lauryl-L-PheZ **17b**: 83.0% yield; mp 113—114 °C (from ether/MeOH); *Rf* (A) 0.81; FAB-MS (nitrobenzyl alchohol) *m/z* 467 (M^++1).

The following compounds, **18b**, **19b** were prepared from the corresponding Z-protected amino acid with similarly to the above described method. Lauryl-L-Phe–L-PheZ **18b**: 93.5% yield; mp 134—134 °C (from MeOH); *Rf* (A) 0.73; HR-FAB-MS (nitrobenzyl alchohol) *m/z* 614 (M^++1): mass found 614.3951, Calcd for $C_{38}H_{52}N_3O_4$ 614.3961. Lauryl-L-Phe–L-Phe–L-LeuZ **19b**: 85.7% yield; mp 170—173 °C (from ether/$CHCl_3$); *Rf* (A) 0.64; HR-FAB-MS (nitrobenzyl alchohol) *m/z* 727 (M^++1): Found 727.4794, Calcd for $C_{44}H_{63}N_4O_5$ 727.4801.

Deprotection. Synthesis of the 1,12-Dodecano-bis(L-Phe) (6a) 5a (3.80 g, 4.98 mmol) was dissolved, by heating on a water bath, in MeOH/DMF (120 ml/30 ml). A slurry consisting of 5% Pd/C (0.75 g) was added, and the mixture was shaken in a hydrogen atomosphere. The catalyst was removed by filtration, and the filtrate and washings were combined and evaporated. The residue crystallized with water in an ice bath, to afford **6a** (2.61 g, 87.8%) of colorless crystals: *Rf* (A) 0.23: mp 116—117 °C (from ether/$CHCl_3$). $[\alpha]_D^{21}$ +22.8 (*c*=0.264, MeOH). ^{1}H-NMR (signal assignments from the spectra of H–H COSY at 500 MHz, $CDCl_3$) δ 1.19—1.28 (m, 10H, –(CH_2)–×5), 2.58—2.81 (dd, 1H, *J*=9.0, 13.6 Hz, Phe C$^\beta$H), 3.19—3.37 (m, 3H, –C^{1}H$_2$– and Phe C$^\beta$H), 3.53—3.67 (dd, 1H, *J*=4.4, 9.5 Hz, Phe C$^\alpha$H), 7.24 (br s, 1H, –NHCO–), 7.24—7.25 (m, 5H, Ar-H). ^{13}C-NMR (signal assignments from the spectra of C–H COSY at 500 Mz, $CDCl_3$) ppm 26.95 (C3), 29.24 (C4, 5, 6), 29.53 (C2), 39.10 (C1), 41.16 (Phe C$^\beta$), 56.48 (Phe C$^\alpha$), 126.70 (*p*), 128.58 (*o*), 129.22 (*m*), 138.03 (*t*), 173.90 (–NHCO–). IR (KBr) cm^{-1}; 3270, 1640; HR-MS *m/z*: Found 494.3606. Calcd for $C_{30}H_{46}N_4O_2$ 494.3618.

The following compounds, **6a**—**10h** were prepared from the corresponding Z(or Boc)-protected amino acid with similarly to the above described method. 1,12-Dodecano-bis(L-Phe) **6a**: 97.0% yield; mp 116—117 °C (from ether/$CHCl_3$); *Rf* (A) 0.23. 1,12-Dodecano-bis(L-Ile) **6b**: 92.0% yield; mp 83—84 °C (from MeOH); *Rf* (A) 0.23. 1,12-Dodecano-bis(D-Phe) **6c**: 94.7% yield; mp 115—116 °C (from ether/MeOH); *Rf* (A) 0.20. 1,12-Dodecano-bis(L-Leu)**6d**: 87.0% yield; mp 95—97 °C (from hexane/$CHCl_3$); *Rf* (A) 0.14. 1,12-Dodecano-bis(L-Phe–L-Phe) **8a**: 82.8% yield; mp 120—122 °C (from MeCN); *Rf* (B) 0.49. 1,12-Dodecano-bis(L-Ile–L-Ile) **8b**: 89.3% yield; mp 122—124 °C (from ether/$CHCl_3$); *Rf* (A) 0.23. 1,12-Dodecano-bis(L-Phe–L-Val) **8c**: 90.5% yield; mp 144—146 °C (from ether/$CHCl_3$); *Rf* (B) 0.43. 1,12-Dodecano-bis(L-Ile–L-Phe) **8d**: 87.0% yield; mp 125—126 °C (from ether/MeOH); *Rf* (B) 0.46. 1,12-Dodecano-bis(D-Phe–L-Phe) **8e**: 73.8% yield; mp 102—104 °C (from ether/MeOH); *Rf* (B) 0.41. 1,12-Dodecano-bis(L-Phe–D-Phe) **8f**: 75.0% yield; mp 115—116 °C (from ether/$CHCl_3$); *Rf* (B) 0.42. 1,12-Dodecano-bis(D-Phe–D-Phe) **8g**: 74.7% yield; mp 128—129 °C (from MeCN); *Rf* (B) 0.50. 1,12-Dodecano-bis(L-Leu–L-Phe) **8h**: 76.0% yield; mp 68—70 °C (from MeCN); *Rf* (B) 0.48. 1,12-Dodecano-bis(L-Phe–L-Phe–L-Leu) **10a**: 71.8% yield; mp 186—188 °C (from ether/$CHCl_3$); *Rf* (B) 0.30. 1,12-Dodecano-bis(L-Phe–L-Phe–L-Val) **10b**: 81.0% yield; mp 215—217 °C (from ether/$CHCl_3$); *Rf* (B) 0.27. 1,12-Dodecano-bis(L-Phe–L-Phe–L-Ile) **10c**: 79.5% yield; mp 127—129 °C (ether/$CHCl_3$); *Rf* (A) 0.23. 1,12-Dodecano-bis(L-Phe–L-Val–L-Leu) **10d**: 86.5% yield; mp 214—217 °C (from MeOH/$CHCl_3$/ether); *Rf* (B) 0.31. 1,12-Dodecano-bis(L-Ile–L-Phe–L-Leu) **10e**: 91.8% yield; mp 161—163 °C (from ether/$CHCl_3$); $[\alpha]_D^{23}$ −19.1 (*c*=0.300, MeOH); *Rf* (B) 0.30. 1,12-Dodecano-bis(L-Leu–L-Leu–L-Phe) **10f**: 90.5% yield; mp 104—106 °C (from MeOH); *Rf* (B) 0.54. 1,12-dodecano-bis(L-Leu–L-Phe–L-Phe) **10g**: 93.5% yield; mp 210—213 °C (dec.) (from ether/MeOH); *Rf* (B)=0.54. 1,12-Dodecano-bis(D-Phe–D-Phe–D-Leu) **10h**: 66.3% yield; mp 188—190 °C (from ether/$CHCl_3$); *Rf* (B) 0.32; FAB-MS (nitrobenzyl alchohol) *m/z* 1016 (M^++1).

Synthesis of 1,12-Dodecano-bis(D-Phe–D-Phe) (8g) To N_α-Boc protected **7g** (2.00 g, 1.9 mmol) anhydrous TFA (12 ml) was added dropwise over a period of 0.5 min. The mixture was stirred at 4 °C for 80 min, and then was poured into ice/water, and adjusted to pH 7—8 with 5% $NaHCO_3$ and 1 M NaOH. The resulting solid was collected, washed with water, and dried *in vacuo*: 74.7% yield. The product was purified with silica gel (35 g) column chromatography eluting with $CHCl_3$ and 3% MeOH/$CHCl_3$ (stepwise elution) to give **8g** as colorless crystals: mp 128—129 °C (from ether/MeOH); TLC *Rf* (B) 0.50. ^{1}H-NMR(signal assignments from the spectra of H–H COSY at 500 Mz, $CDCl_3$/DMSO-d_6) δ 1.21—1.37 (m, 10H, –(CH_2)–×5), 2.58 (dd, 1H, *J*=8.9, 13.2 Hz, Phe^2 C$^\beta$H), 2.91 (dd, 1H, *J*=7.6, 13.4 Hz, Phe^1 C$^\beta$H), 3.02 (dd, *J*=5.2, 12.8 Hz, Phe^2 C$^\beta$H), 3.06—3.12 (m, 3H, –C^{1}H$_2$–, Phe^1 C$^\beta$H), 3.49 (dd, 1H, *J*=4.3, 9.2 Hz, Phe^2 C$^\alpha$H), 4.61 (dd, 1H, *J*=7.6, 14.3 Hz, Phe^1 C$^\alpha$H), 7.14—7.31 (m, 10H, Ar-H), 7.45 (t, 1H, *J*=5.2 Hz, –NH^{a}CO–), 7.95 (d, 1H, *J*=8.2 Hz, nNH^{b}CO–). ^{13}C-NMR ($CDCl_3$/DMSO-d_6) ppm 26.65 (C3), 29.05 (C6), 29.14 (C4), 29.28 (C2, 5), 38.09 (C1), 38.20 (Phe^1 C$^\beta$), 39.07 (Phe^2 C$^\beta$), 54.50 (Phe^2 C$^\alpha$), 54.78 (Phe^1 C$^\alpha$), 126.38 (*p*), 126.90 (*p'*), 128.11 (*o*), 128.41 (*o'*), 129.30 (*m*), 129.47 (*m'*), 135.62 (*t*), 137.34 (*t'*), 169.55 (–NH^{a}CO–), 170.37 (–NH^{b}CO–); IR (KBr) 3270, 1630 cm^{-1}; FAB-MS (nitrobenzyl alchohol) *m/z* 790 (M^++1).

1,12-Dodecano-bis(L-Ile) (**6b**): Colorless solid; $[\alpha]_D^{21}$ +10.4 (*c*=0.156, MeOH); ^{1}H-NMR ($CDCl_3$) δ 0.88 (t, 3H, *J*=7.0 Hz, Ile C$^\delta$H$_3$), 0.94 (d, 3H, *J*=7.0 Hz, Ile C$^\gamma$H$_3$), 1.20—1.40 (m, 10H, –(CH_2)–×5), 1.40—1.56 (m, 2H, Ile C$^\gamma$H$_2$), 1.88—2.04 (m, 1H, Ile C$^\beta$H), 3.15—1.33 (m, 3H, Ile C$^\alpha$H, –C^{1}H$_2$–), 7.24 (br, 1H, –NHCOn–); ^{13}C-NMR ($CDCl_3$) ppm 11.92 (Ile C$^\delta$), 16.26 (Ile C$^{\gamma'}$), 23.78 (C3), 27.01 (Ile C$^\gamma$), 29.29 (C6) , 29.53 (C4, C5), 29.71 (C2), 38.04 (Ile C$^\beta$), 39.04 (C1), 60.00 (Ile C$^\alpha$), 174.07 (–NHCO–); IR (KBr) 3270, 1630 cm^{-1}.

1,12-Dodecano-bis(L-Phe–L-Phe) (**8a**): Colorless solid; $[\alpha]_D^{21}$ +5.5 (*c*= 0.319, MeOH); ^{1}H-NMR (signal assignments from the spectra of H–H COSY at 500 Mz, $CDCl_3$) δ 1.21—1.37 (m, 10H, –(CH_2)–×5), 2.56 (dd, 1H, *J*=9.5, 14.0 Hz, Phe^2 C$^\beta$H), 3.03—3.21 (m, 4H, –C^{1}H$_2$–, Phe^1 C$^\beta$H, Phe^2 C$^\beta$H), 3.55 (dd, 1H, *J*=4.0, 9.5 Hz, Phe^2 C$^\alpha$H), 4.62 (dd, 1H, *J*=7.8, 15.7 Hz, Phe^1 C$^\alpha$H), 6.21 (t, 1H, *J*=5.4 Hz, –NH^{a}CO–), 7.14—7.33 (m, 10H, Ar-H), 7.88 (d, 1H, *J*=8.4 Hz, –NH^{b}CO–); ^{13}C-NMR (signal assignments from the spectra of C–H COSY at 500 Mz, $CDCl_3$): ppm 26.77 (C3), 29.19 (C6), 29.28 (C4), 29.41 (C5), 29.47 (C2), 38.36 (C1), 39.49 (Phe^1 C$^\beta$), 40.71 (Phe^2 C$^\beta$), 54.33 (Phe^2 C$^\alpha$), 56.27 (Phe^1 C$^\alpha$), 126.87 (*p*, *p'*), 128.52 (*o'*), 128.72 (*o*), 129.23 (*m'*), 129.34 (*m*), 136.91 (*t'*), 137.56 (*t*), 170.63 (–NH^{a}CO–), 174.50 (–NH^{b}CO–); IR (KBr) 3280, 1635 cm^{-1}; FAB-MS (nitrobenzyl alchohol) *m/z* 789 (M^++1). *Anal.* Calcd for $C_{48}H_{64}N_6O_4 \cdot 1/2H_2O$ (798.0838): C, 72.24; H, 8.21; N, 10.53. Found: C, 72.46; H, 8.14; N, 10.48.

1,12-Dodecano-bis(L-Ile–L-Ile) (**8b**): Colorless solid; $[\alpha]_D^{21}$ −22.4 (*c*=

0.154, MeOH); ^{1}H-NMR ($CDCl_3$) δ 0.88—0.99 (overlap, 12H, $CH_3\times4$), 1.25—1.54 (m, 14H, $-(CH_2)-\times5$), 1.90—1.98 (m, 2H, Ile^1 C$^\beta$H, Ile^2 C$^\beta$H), 3.15—3.28 (m, 3H, $-C^1H_2-$, Ile^2 C$^\alpha$H), 4.17 (dd, 1H, J=6.8, 9.0 Hz, Ile^1 C$^\alpha$H), 6.40 (m, 1H, $-NH^aCO-$), 7.88 (d, 1H, J=9.0 Hz, $-NH^bCO-$); ^{13}C-NMR ($CDCl_3$) ppm 11.09 (Ile^1 Me), 11.92 (Ile^2 Me), 15.62 (Ile^1 Me), 16.14 (Ile^2 Me), 23.95 (C3, 4, 5, 6), 25.01 (Ile^1 C$^\gamma$), 26.95 (Ile^2 C$^\gamma$), 29.30 (C2), 36.75 (Ile^1 C$^\beta$), 38.16 (C1), 39.45 (Ile^2 C$^\beta$), 57.59 (Ile^1 C$^\alpha$), 60.00 (Ile^2 C$^\alpha$), 171.26 ($-NH^aCO-$), 174.54 ($-NH^bCO-$); IR (KBr) 3270, 1630 cm^{-1}; FAB-MS (nitrobenzyl-alchohol) m/z 654 (M^++1).

1,12-Dodecano-bis(L-Phe–L-Val) (**8c**): Colorless solid; ^{1}H-NMR ($CDCl_3$/DMSO-d_6) δ 0.67 (d, 3H, J=6.8 Hz, Val CH_3), 0.86 (d, 3H, J=6.8 Hz, Val CH_3), 1.18—1.38 (m, 10H, $-(CH_2)-\times5$), 2.03 (m, 1H, Val C$^\beta$H), 2.92 (dd, 1H, J=8.3, 13.7 Hz, Phe C$^\beta$H), 3.06—3.15 (m, 4H, $-C^1H_2-$ and Phe C$^\beta$H), 3.15—3.25 (m, 1H, Val C$^\alpha$H), 4.63 (dd, 1H, J=8.3, 14.4 Hz, Phe C$^\alpha$H), 7.10—7.25 (m, 5H, Ar-H), 7.53 (m, 1H, $-NH^aCO-$), 8.02 (d, 1H, J=8.3 Hz, $-NH^bCO-$); ^{13}C-NMR (DMSO-d_6/$CDCl_3$) ppm 16.33 (Val CH_3), 19.39 (Val CH_3), 26.61 (C3), 29.01 (Val C$^\beta$), 29.12 (C4, 5, 6), 29.23 (C2), 30.80 (C1), 38.43 (Phe C$^\beta$), 38.99 (Val C$^{\beta'}$), 53.76 (Val C$^\alpha$), 59.82 (Phe C$^\alpha$), 126.32 (p), 128.05 (o), 129.18 (m), 137.29 (i), 170.80 ($-NH^aCO-$), 173.64 ($-NH^cCO-$); IR (KBr) 3280, 1630 cm^{-1}.

1,12-Dodecano-bis(L-Ile–L-Phe) (**8d**): Colorless solid; $[\alpha]_D^{23}$ −30.2 (c=0.344, MeOH); ^{1}H-NMR ($CDCl_3$) δ 0.87—0.94 (m, 6H, Ile Me×2), 1.24—1.04 (m, 14H, $-(CH_2)-\times7$), 3.63 (m, 1H, Phe C$^\alpha$H), 4.16 (dd, 1H, J=8.3, 14.0 Hz, Ile C$^\alpha$H), 6.25 (t, 1H, J=5.3 Hz, $-NH^aCO-$), 7.24—7.26 (m, 5H, Ar-H), 7.86 (d, 1H, J=9.0 Hz, $-NH^bCO-$); ^{13}C-NMR ($CDCl_3$) ppm 11.21 (Ile Me), 15.61 (Ile Me), 25.01 (Ile C$^\gamma$), 29.41 (C4, 5, and 6), 33.99 (C2), 36.87 (C1), 39.51 (Ile C$^\beta$), 41.04 (Phe C$^\beta$), 56.48 (Phe C$^\alpha$), 57.77 (Ile C$^\alpha$), 126.81 (p), 128.59 (o), 129.28 (m), 137.67 (i), 171.08 ($-NH^aCO-$), 174.37 ($-NH^bCO-$); IR (KBr) 3260, 1630 cm^{-1}; HR-FAB-MS m/z [M^+, $C_{42}H_{68}N_6O_4$] Calcd 720.5301, Found 720.5346. *Anal.* Calcd for $C_{42}H_{68}N_6O_4\cdot1/2H_2O$: C, 69.10; H, 9.53; N, 11.51. Found: C, 69.33; H, 9.28; N, 11.50.

1,12-Dodecano-bis(D-Phe–L-Phe) (**8e**): Colorless solid; ^{1}H-NMR (signal assignments from the spectra of H–H COSY at 500 Mz, $CDCl_3$/DMSO-d_6) δ 1.21—1.37 (m, 10H, $-(CH_2)-\times5$), 2.58 (dd, 1H, J=8.9, 13.2 Hz, Phe^2 C$^\beta$H), 2.91 (dd, 1H, J=7.6, 13.4 Hz, Phe^1 C$^\beta$H), 3.02 (dd, J=5.2, 12.8 Hz, Phe^2 C$^\beta$H), 3.06—3.12 (m, 3H, $-C^1H_2-$, Phe^1 C$^\beta$H), 3.49 (dd, 1H, J=4.3, 9.2 Hz, Phe^2 C$^\alpha$H), 4.61 (dd, 1H, J=7.6, 14.3 Hz, Phe^1 C$^\alpha$H), 7.14—7.31 (m, 10H, Ar-H), 7.45 (t, 1H, J=5.2 Hz, $-NH^aCO-$), 7.95 (d, 1H, J=8.2 Hz, $-NH^bCO-$). ^{13}C-NMR ($CDCl_3$/DMSO-d_6) ppm 26.62 (C3), 29.02 (C6), 29.11 (C4), 29.25 (C5), 29.28 (C2), 38.32 (C1), 38.98 (Phe^1 C$^\beta$), 40.94 (Phe^2 C$^\beta$), 53.85 (Phe^2 C$^\alpha$), 56.20 (Phe^1 C$^\alpha$), 126.26 (p), 126.32 (p'), 128.02 (o), 128.21 (o'), 129.15 (m), 129.22 (m'), 137.26 (ι), 138.18 (ι'), 170.65 ($-NH^aCO-$), 174.02 ($-NH^bCO-$); IR (KBr) 3280, 1630 cm^{-1}; FAB-MS (nitrobenzyl alchohol) m/z 790 (M^++1).

1,12-Dodecano-bis(L-Phe–D-Phe) (**8f**): Colorless solid; ^{1}H-NMR (signal assignments from the spectra of HOM spin decoupling at 500 Mz, $CDCl_3$/DMSO-d_6) δ 1.20—1.40 (m, 10H, $-(CH_2)-\times5$), 2.72 (dd, 1H, J=7.6, 14.0 Hz, Phe^2 C$^\beta$H), 2.83 (dd, 1H, J=9.5, 13.7 Hz, Phe^1 C$^\beta$H), 2.92 (dd, J=5.5, 14.0 Hz, Phe^2 C$^\beta$H), 3.06—3.14 (m, 3H, $-C^1H_2-$, Phe^1 C$^\beta$H), 4.05 (dd, 1H, J=5.5, 7.3 Hz, Phe^2 C$^\alpha$H), 4.59 (dd, 1H, J=5.0, 8.9 Hz, Phe^1 C$^\alpha$H), 7.14—7.31 (m, 10H, Ar-H), 7.78 (br, 1H, $-NH^aCO-$), 8.73 (d, 1H, J=8.5 Hz, $-NH^bCO-$). ^{13}C-NMR ($CDCl_3$/DMSO-d_6) ppm 26.63 (C3), 29.03 (C6), 29.15 (C4), 29.26 (C2, 5), 37.88 (C1), 38.20 (Phe^1 C$^\beta$), 39.10 (Phe^2 C$^\beta$), 54.37 (Phe^2 C$^\alpha$), 54.58 (Phe^1 C$^\alpha$), 126.43 (p), 126.88 (p'), 128.08 (o), 128.37 (o'), 129.27 (m), 129.44 (m'), 135.41 (i), 137.47 (ι'), 169.38 ($-NH^aCO-$), 170.54 ($-NH^bCO-$); IR (KBr) 3280, 1630 cm^{-1}; FAB-MS (nitrobenzyl alchohol) m/z 790 (M^++1).

1,12-Dodecano-bis(L-Phe–L-Phe–L-Leu) (**10a**): Colorless solid; $[\alpha]_D^{21}$ −22.4 (c=0.078, MeOH). ^{1}H-NMR (signal assignments from the spectra of H–H COSY at 500 Mz, $CDCl_3$) δ 0.86 (d, 3H, J=10.4 Hz, Leu Me), 0.88 (d, 3H, J=10.4 Hz, Leu Me), 1.11—1.36 (m, 10H, $-(CH_2)-\times5$), 1.50—1.58 (m, 1H, Leu C$^\gamma$H), 2.85—3.04 (m, 2H, Phe^2 C$^\beta$H), 3.06—3.19 (m, 7H, $-C^1H_2-$, Leu C$^\beta$H, Phe^1 C$^\beta$H, Phe^2 C$^\beta$H), 4.58 (m, 3H, J=7.4, 8.4 Hz, Leu C$^\alpha$H, Phe^1 C$^\alpha$H, Phe^2 C$^\alpha$H), 6.08 (br s, 1H, $-NH^aCO-$), 6.59 (d, 1H, J=8.4 Hz, $-NH^bCO-$), 7.04—7.31 (m, 10H, Ar-H), 7.82 (d, 1H, J=7.4 Hz, $-NH^cCO-$); ^{13}C-NMR (signal assignments from the spectra of C–H COSY at 500 Mz, $CDCl_3$) ppm 21.48 (Leu Me), 23.25 (Leu Me), 24.83 (C3), 26.83 (Leu C$^\gamma$), 29.24 (C4, 5, 6), 29.47 (C2), 37.52 (C1), 37.87 (Leu C$^\beta$), 39.69 (Phe^1 C$^{\beta'}$), 43.80 (Phe^2 C$^{\beta'}$), 53.43 (Leu C$^\alpha$), 54.13 (Phe^2 C$^{\alpha'}$), 54.25 (Phe^1 C$^\alpha$), 126.70 (p), 127.00 (p'), 128.46 (o), 128.58 (o'), 129.28 (m), 129.40 (m'), 136.56 (ι), 136.79 (ι'), 170.14 ($-NH^aCO-$), 170.73 ($-NH^bCO-$), 176.13 (nNH^cCO-); IR (KBr) 3280, 1630 cm^{-1}; FAB-MS (nitrobenzyl alchohol) m/z 1016 (M^++1). *Anal.* Calcd for $C_{60}H_{86}N_8O_6\backslash1/2H_2O$: C, 70.35; H, 8.56; N, 10.94. Found: C, 70.61; H, 8.49; N, 11.00.

1,12-Dodecano-bis(L-Phe–L-Phe–L-Val) (**10b**): Colorless solid; ^{1}H-NMR ($CDCl_3$/DMSO-d_6) δ 0.86 (d, 3H, J=6.7 Hz, Val Me), 0.90 (d, 3H, J=7.0 Hz, Val Me), 1.15—1.35 (m, 10H, $-(CH_2)-\times5$), 2.11 (m, 1H, Val C$^\beta$H), 2.88—2.96 (m, 1H, Phe^2 C$^\beta$H), 3.01—3.28 (m, 5H, $-C^1H_2-$, Phe^1 C$^\beta$H, Phe^2 C$^\beta$H), 3.58 (d, 1H, J=5.2 Hz, Val C$^\alpha$H), 4.52—4.67 (m, 2H, Phe^1 C$^\alpha$H, Phe^2 C$^\alpha$H), 7.14—7.26 (m, 10H, Ar-H), 7.96 (d, 1H, J=8.2 Hz, $-NH^bCO-$), 8.57 (d, 1H, J=7.9 Hz, $-NH^cCO-$); ^{13}C-NMR ($CDCl_3$/DMSO-d_6) ppm 16.03 (Val Me), 19.43 (Val Me), 26.71 (C3), 29.12 (C4, 5, 6), 29.34 (C2), 30.71 (Val C$^\beta$), 37.75 (C1), 39.10 (Phe^1, Phe^2 C$^\beta$), 54.01 (Val C$^\alpha$), 56.24 (Phe^2 C$^\alpha$), 60.06 (Phe^1 C$^\alpha$), 126.40 (p), 128.11 (o), 128.22 (o'), 129.10 (m), 129.22 (m'), 136.85 (ι), 137.15 (ι'), 170.26 ($-NH^aCO-$), 170.61 ($-NH^bCO-$), 174.66 ($-NHCCO-$); IR (KBr) 3270, 1630 cm^{-1}; FAB-MS (nitrobenzyl alchohol) m/z 988(M^++1).

1,12-Dodecano-bis(L-Phe–L-Val–L-Leu) (**10d**): Colorless solid; $[\alpha]_D^{21}$ −27.3 (c=0.172, MeOH); ^{1}H-NMR ($CDCl_3$/DMSO-d_6) δ 0.78 (d, 3H, J=6.7 Hz, Val Me), 0.83 (d, 3H, J=6.7 Hz, Val Me), 0.93 (t, 6H, J=6.7 Hz, Leu Me×2), 1.18—1.41 (m, 10H, $-(CH_2)-\times5$), 1.55 (m, 2H, Val C$^\beta$H$_2$), 1.75 (m, 1H, Leu C$^\gamma$H), 2.03 (m, 1H, Val C$^\beta$H), 2.91 (dd, 1H, J=8.5, 14.0 Hz, Phe C$^\beta$H), $-(CH_2)-\times2$), 3.05—3.15 (overlap, 3H, $-C^1H_2-$, Phe C$^\beta$H), 3.44 (dd, 1H, J=4.8, 9.4 Hz, Leu C$^\alpha$H), 4.16 (dd, 1H, J=6.7, 8.5 Hz, Val C$^\alpha$H), 4.60 (dd, 1H, J=8.5, 14.3 Hz, Phe C$^\alpha$H), 7.18—7.23 (m, 5H, Ar-H), 7.38 (t, 1H, J=5.5 Hz, $-NH^aCO-$), 7.76 (d, 1H, J=8.5 Hz, $-NH^bCO-$), 8.01 (d, 1H, J=8.5 Hz, $-NHCCO-$); ^{13}C-NMR ($CDCl_3$/DMSO-d_6) ppm 17.76 (Ile Me), 19.19 (Ile Me), 21.48 (Leu Me), 23.23 (Leu Me), 24.34 (Leu C$^\gamma$), 26.62 (C3), 29.02 (C4), 29.06 (C5), 29.23 (C6), 29.28 (C2), 30.47 (Val C$^\beta$), 37.73 (C1), 39.09 (Leu C$^\beta$), 43.18 (Phe C$^\beta$), 53.04 (Leu C$^\alpha$), 54.09 (Phe C$^\alpha$), 58.09 (Val C$^\alpha$), 126.26 (p), 128.03 (o), 129.15 (m), 137.44 (Ar-C), 170.62 ($-NH^aCO-$), 170.84 ($-NH^bCO-$), 174.70 ($-NHCCO-$); IR (KBr) 3280, 1630 cm^{-1}; FAB-MS (nitrobenzyl alchohol) m/z 920 (M^++1).

1,12-Dodecano-bis(L-Leu–L-Leu–L-Phe) (**10f**): Colorless solid; $[\alpha]_D^{21}$ −44.0 (c=0.217, MeOH); ^{1}H-NMR ($CDCl_3$) δ 0.87—0.92 (overlap, 12H, Leu Me×4), 1.20—1.30 (m, 10H, $-(CH_2)-\times5$), 1.52—1.74 (m, 6H, Leu C$^\gamma$H$_2\times2$, Leu C$^\beta$H×2), 2.74 (dd, 1H, J=9.2, 13.7 Hz, Phe C$^\beta$H), 3.18—3.22 (m, 3H, $-C^1H_2-$, Phe C$^\beta$H), 3.64 (dd, 1H, J=4.0, 9.2 Hz, Phe C$^\alpha$H), 4.39—4.47 (overlap, 2H, Leu^1 C$^\alpha$H, Leu^2 C$^\alpha$H), 6.58 (t, 1H, J=5.5 Hz, $-NH^aCO-$), 6.96 (d, 1H, J=8.4 Hz, $-NH^bCO-$), 7.19—7.31 (m, 5H, Ar-H), 7.78 (d, 1H, J=9.3 Hz, $-NHCCO-$); ^{13}C-NMR ($CDCl_3$) ppm 22.02 (Leu Me), 22.19 (Leu Me), 22.87 (Leu Me), 22.98 (Leu Me), 24.81 (Leu C$^\gamma$), 24.86 (Leu C$^\gamma$), 26.83 (C3), 29.15, 29.35, 29.41 (C2), 39.59 (C1), 40.74 (Leu C$^\beta\times2$, 40.82 (Phe C$^\beta$), 51.85 (Leu1 C$^\alpha$), 51.89 (Leu^2 C$^\alpha$), 56.18 (Phe^1 C$^\alpha$), 126.90 (p), 128.72 (o), 129.32 (m), 137.48 (ι), 171.60 ($-NH^aCOn$), 172.16 ($-NH^bCO-$), 174.70 ($-NHCCO-$); IR (KBr) 3260, 1630 cm^{-1}. FAB-MS (nitrobenzyl alchohol) m/z 948 (M^++1).

1,12-Dodecano-bis(L-Leu–L-Phe–L-Phe) (**10g**): Color less solid; ^{1}H-NMR ($CDCl_3$/DMSO-d_6) δ 0.89 (d, 3H, J=6.4 Hz, Leu Me), 0.93 (d, 3H, J=6.4 Hz, Leu Me), 1.53 (m, 2H, Leu C$^\beta$H×2), 1.64 (m, 1H, Leu C$^\gamma$H), 2.93 (dd, 1H, J=8.8, 14.3 Hz, Phe^2 C$^\beta$H), 2.98 (dd, 1H, J=8.8, 14.3 Hz, Phe^3 C$^\beta$H), 3.07 (dd, 2H, J=6.4, 13.4 Hz, $-C^1H_2-$), 3.11 (dd, 1H, J=5.5, 13.7 Hz, Phe^2 C$^\beta$H), 3.20 (dd, 1H, J=5.2, 14.3 Hz, Phe^3 C$^\beta$H), 4.07 (dd, 1H, J=5.0, 8.0 Hz, Phe^3 C$^\alpha$H), 4.36 (ddd, 1H, J=5.8, 8.24, 14.6 Hz, Phe^1 C$^\alpha$H), 4.66 (ddd, 1H, J=5.8, 8.24, 13.7 Hz, Phe^2 C$^\alpha$H), 7.17—7.28 (m, 10H, Ar-H), 7.38 (t, 1H, J=5.5 Hz, $-NH^aCO-$), 8.07 (t, 1H, J=8.2 Hz, $-NH^bCO-$), 8.86 (t, 1H, J=8.2 Hz, $-NHCCO-$). ^{13}C-NMR ($CDCl_3$/DMSO-d_6) ppm 21.88 (Leu Me), 22.97 (Leu Me), 24.46 (C3), 26.63 (Leu C$^\gamma$), 29.02 (C4), 29.17 (C5), 29.26 (C2, 6), 37.18 (Leu^1 C$^\beta$), 37.76 (C1), 39.03 (Phe^2 C$^\beta$), 41.26 (Phe^3 C$^\beta$), 51.72 (Leu^1 C$^\alpha$), 53.89 (Phe^2 C$^\alpha$), 54.92 (Phe^3 C$^\alpha$), 126.41 (p), 127.14 (p'), 128.14 (o), 128.50 (o'), 129.33 (m), 129.57 (m'), 134.77 (ι), 137.23 (ι'), 168.25 ($-NH^aCO-$), 170.25 ($-NH^bCO-$), 171.76 ($-NHCCO-$); FAB-MS (nitrobenzyl alchohol) m/z 1016 (M^++1).

1,2-Ethano-bis(L-Phe) **12a**: 93.0% yield; mp 116—118 °C (from ether/MeOH); Rf (B) 0.26. 1,2-Ethano-bis(L-Leu) **12b**: 96.7% yield; oil; Rf (B) 0.26. 1,2-Ethano-bis(D-Leu) **12c**: 89.8% yield; mp 97—98 °C; Rf (B) 0.22. 1,2-Ethano-bis(L-Phe–L-Phe) **14a**: 98.0% yield; mp 206—208 °C; Rf (B) 0.44. 1,2-Ethano-bis(L-Phe–D-Phe) **14b**: 95.0% yield; mp 203—206 °C; Rf (B) 0.21. 1,2-Ethano-bis(L-Phe–L-Phe–L-Leu) **16a**: 95.0% yield; mp 249—250 °C (from MeOH); Rf (B) 0.48. 1,2-Ethano-bis(L-Phe–L-Phe–L-Val) **16b**: 94.7% yield; mp 249—251 °C (from MeOH); TLC Rf (B) 0.33.

Synthesis of 1,2-Ethano-bis(L-Phe–L-Phe–L-Val) (16b) To N$_\alpha$-Boc protected **15b** (0.732 g, mmol) anhydrous TFA (6 ml) was added dropwise over a period of 0.5 min. The mixture was stirred at 4 °C for 60 min, and then was poured into ice/water, and adjusted to pH 7 with 5% $NaHCO_3$. The resulting solid was collected, washed with water, and dried *in vacuo*: 94.7% yield. The product was purified with silica gel (50 g) column chromatogra-

phy eluting with 2% MeOH/$CHCl_3$ and 10% MeOH/$CHCl_3$ (stepwise elution) to give **16b** as a colorless crystals: mp 249—251 °C (from MeOH); TLC *Rf* (B) 0.33; ^{1}H-NMR ($CDCl_3$/DMSO-d_6) δ 0.586 (d, 3H, J=6.7 Hz, Val Me), 0.777 (d, 3H, J=6.7 Hz, Val Me), 1.90 (m, 1H, Val C$^{\beta}$H), 2.81 (dd, 1H, J=5.0, 13.7 Hz, Phe^2 C$^{\beta}$H), 2.88 (dd, 1H, J=8.6, 13.7 Hz, Phe^1 C$^{\beta}$H), 2.99 (d, 2H, J=4.9 Hz, Phe C$^{\beta}$H), 3.02 (dd, 1H, J=5.5, 9.0 Hz, Val C$^{\alpha}$H), 3.08 (m, 2H, –C^{1}H$_2$–), 4.48 (ddd, 1H, J=5.5, 8.3, 8.3 Hz, Phe^2 C$^{\alpha}$H), 4.59 (m, 1H, Phe^1 C$^{\alpha}$H), 7.13—7.25 (m, 10H, Ar-H), 7.73 (br s, 1H, –NH^{a}CO–), 7.96 (br s, 1H, –NH^{b}CO–), 8.07 (d, 1H, J=8.2 Hz, –NH^{c}CO–); ^{13}C-NMR ($CDCl_3$/DMSO-d_6) ppm 16.76 (Val Me), 19.80 (Val Me), 31.19 (Val C$^{\beta}$), 38.03 (C1), 38.80 (Phe C$^{\beta}$), 39.19—41.24 (Leu and Phe C$^{\beta}$, overlap with DMSO-d_6), 53.97 (Val C$^{\alpha}$), 54.58 (Phe^2 C$^{\alpha}$), 60.37 (Phe^1 C$^{\alpha}$), 126.58 (*p*), 128.35 (*o*), 129.56 (*m*), 137.75 (*i*), 137.93 (*i'*), 171.21 (–NH^{a}CO–), 171.30 (–NH^{b}CO–), 174.70 (–NH^{c}CO–); FAB-MS (nitrobenzyl alchohol) *m/z* 848 (M^++1).

1,2-Ethano-bis(L-Phe–L-Phe) (**14a**): Colorless solid; ^{1}H-NMR ($CDCl_3$) δ 2.44 (dd, 1H, J=9.5, 13.7 Hz, Phe^2 C$^{\beta}$H), 2.98 (dd, 1H, J=7.3, 13.6 Hz, –C^{1}H$_1$–), 3.05 (dd, 1H, J=7.3, 13.4 Hz, –C^{1}H$_1$–), 3.08 (m, 1H, Phe^1 C$^{\beta}$H), 3.10 (dd, 1H, J=3.7, 13.7 Hz, Phe^2 C$^{\beta}$-H), 3.19 (m, 1H, Phe^1 C$^{\beta}$H), 3.61 (dd, 1H, J=3.7, 9.6 Hz, Phe^2 C$^{\alpha}$H), 4.50 (ddd, 1H, J=7.6, 7.8, 7.8 Hz, Phe^1 C$^{\alpha}$H), 6.23 (br s, 1H, –NH^{a}CO–), 7.14—7.17, 7.28—7.32 (m, 10H, Ar-H), 7.77 (d, 1H, J=8.2 Hz, –NH^{b}CO–); ^{13}C-NMR ($CDCl_3$) ppm 38.1 (C1), 39.4 (Phe^1 C$^{\beta}$), 40.7 (Phe^2 C$^{\beta}$), 54.2 (Phe^2 C$^{\alpha}$), 56.4 (Phe^1 C$^{\alpha}$), 126.9 (*p*), 127.1 (*p*), 128.7 (*o*), 129.4 (*m*), 136.8 (*i*) and 137.6 (*i'*), 171.6 (–NH^{a}CO–), 174.7 (–NH^{b}CO–); FAB-MS (nitrobenzyl alchohol) *m/z* 650 (M^++1).

1,2-Ethano-bis(L-Phe–D-Phe) (**14b**): Colorless solid; ^{1}H-NMR ($CDCl_3$/DMSO-d_6=0.5/0.2) δ 2.67 (dd, 1H, J=7.9, 14.0 Hz, Phe^2 C$^{\beta}$H), 2.83 (dd, 1H, J=9.5, 13.7 Hz, Phe^1 C$^{\beta}$-H), 2.90 (dd, 1H, J=5.5, 13.7 Hz, Phe^2 C$^{\beta}$H), 3.09 (dd, 1H, J=5.2, 13.7 Hz, Phe^1 C$^{\beta}$-H), 3.20 (m, 2H, –C^{1}H$_2$–), 3.94 (dd, 1H, J=6.1, 7.3 Hz, Phe^2 C$^{\alpha}$H), 4.53 (ddd, 1H, J=5.2, 8.0, 8.9 Hz, Phe^1 C$^{\alpha}$H), 6.99—7.02 (m, 2H, *o*-protons), 7.16—7.24(m, 4H, Ar-H), 7.94 (m, 1H, –NH^{a}CO–), 8.79 (d, 1H, J=8.0 Hz, –NH^{b}CO–); FAB-MS (nitrobenzyl alchohol) *m/z* 650 (M^++1).

1,2-Ethano-bis(L-Phe–L-Phe–L-Leu) (**16a**): Colorless solid; ^{1}H-NMR ($CDCl_3$/DMSO-d_6) δ 0.788 (d, 3H, J=6.7 Hz, Leu Me), 0.824 (d, 3H, J=6.7 Hz, Leu Me), 1.11 (ddd, 1H, J=5.3, 8.9, 13.8 Hz, Leu C$^{\beta}$-H), 1.27 (ddd, 1H, J=5.0, 8.6, 13.6 Hz, Leu C$^{\beta}$H), 1.58 (m, 1H, Leu C$^{\gamma}$H), 2.78 (dd, 1H, J=8.6, 13.7 Hz, Phe^2 C$^{\beta}$H), 2.84 (dd, 1H, J=8.9, 13.7 Hz, Phe^1 C$^{\beta}$H), 2.98 (dd, 2H, J=5.0, 13.6 Hz, Phe^1, Phe^2 C$^{\beta}$H), 3.03 (m, 2H, –C^{1}H$_2$–), 3.18 (dd, 1H, J=5.2, 9.2 Hz, Leu C$^{\alpha}$H), 4.43 (ddd, 1H, J=5.8, 8.2, 8.2 Hz, Phe^1 C$^{\alpha}$H), 4.54 (m, 1H, Phe^2 C$^{\alpha}$H), 7.13—7.27 (m, 10H, Ar-H), 7.93 (t, 1H, J=4.4 Hz, –NH^{a}CO–), 8.06 (br s, 1H, –NH^{b}CO–), 8.25 (d, 1H, J=8.2 Hz, –NH^{c}CO–); ^{13}C-NMR ($CDCl_3$/DMSO-d_6) ppm 21.5, 23.1 (Leu Me), 23.7 (Leu C$^{\gamma}$), 37.6 (Phe C$^{\beta}$), 37.6 (Phe C$^{\beta}$), 38.0 (C1), 43.2 (Leu C$^{\beta}$), 52.6 (Leu C$^{\alpha}$), 54.0 (Phe^1, Phe^2 C$^{\alpha}$), 126.1 (*p*), 126.2 (*p*), 127.8 (*o*), 128.0 (*o*), 129.1 (*m*), 129.2 (*m*), 137.3 (*i*), 137.58 (*i'*), 170.5 (–NH^{a}CO–), 170.7 (–NH^{b}CO–), 174.1 (–NH^{c}CO–); FAB-MS (nitrobenzyl alchohol) *m/z* 898 (MH^++NaI).

The following single-stranded peptides, **17a**—**19a** were prepared from deprotection(Pd/C–H_2 or TFA) of the corresponding Z(or Boc)-protected amino acid similarly to the above described method. Lauryl–L-Phe **17a**: 88.2% yield; mp 51—52 °C (from hexane); *Rf* (B) 0.49. Lauryl–L-Phe–L-PheH (**18a**); 85.0% yield; mp 99—100 °C (from hexane/$CHCl_3$); *Rf* (B) 0.64. Lauryl–L-Phe–L-Phe–L-Leu (**19a**): 67.7% yield; mp 139—140 °C (from hexane/$CHCl_3$); *Rf* (B) 0.50.

Synthesis of the Lauryl–L-Phe–L-PheNH$_2$ (**18a**): Colorless solid: ^{1}H-NMR ($CDCl_3$) δ 0.88 (t, 3H, J=6.8 Hz, Me), 1.25—1.39 (m, 10H, –(CH$_2$)$_{10}$–), 2.49 (dd, 1H, J=9.3, 13.7 Hz, Phe^2 C$^{\beta}$H), 2.95—3.06 (m, 1H, Phe^1 C$^{\beta}$H), 3.10—3.19 (m, 1H, Phe^1 C$^{\beta}$H), 3.10—3.19 (m, 1H, Phe^2 C$^{\beta}$H), 3.10—3.19 (m, 2H, C^{1}H), 3.57 (dd, 1H, J=3.9, 9.3 Hz, Phe^2 C$^{\alpha}$H), 4.56 (dd, 1H, J=8.3, 15.6 Hz, Phe^1 C$^{\alpha}$H), 5.89 (br s, 1H, –NH^{a}CO–), 7.14—7.34 (m, 10H, Ar-H), 7.83 (d, 1H, J=8.3 Hz, –NH^{b}CO–); ^{13}C-NMR ($CDCl_3$) ppm 14.13 (Me), 22.69 (C10, 11), 26.80 (C9), 29.25 (C8), 29.32 (C7), 29.35 (C6), 29.52 (C5), 29.60 (C4), 29.66 (C3), 31.92 (C2), 38.18 (C1), 39.51 (Phe^1 C$^{\beta}$), 40.72 (Phe^2 C$^{\beta}$), 54.46 (Phe^2 C$^{\alpha}$), 56.28 (Phe^1 C$^{\alpha}$), 126.89 (*p*), 128.58 (*o*), 128.73 (*m*), 136.97, 137.58 (Ar-C), 170.54 (–NH^{a}CO–), 174.49 (–NH^{b}CO–); FAB-MS (nitrobenzyl alchohol) *m/z* 480 (M^++1).

Lauryl–L-Phe–L-Phe–L-LeuNH$_2$ (**19a**): Colorless solid: ^{1}H-NMR ($CDCl_3$) δ 0.85 (d, 3H, J=6.4 Hz, Leu Me), 0.88 (m, 3H, Me), 0.89 (d, 3H, J=6.4 Hz, Leu Me), 1.16—1.34 (m, 20H, –(CH$_2$)$_{10}$–), 1.53 (m, 1H, Leu C$^{\gamma}$H), 2.87 (dd, 1H, J=7.0, 13.7 Hz, Phe^2 C$^{\beta}$H), 3.01—3.20 (overlap, 7H, Phe^1 C$^{\beta}$H, Phe^2 C$^{\beta}$H, Leu C$^{\beta}$H, –C^{1}H$_2$–), 4.47—4.62 (overlap, 3H, Phe^1 C$^{\alpha}$H, Phe^2 C$^{\alpha}$H, Leu C$^{\alpha}$H), 5.92 (br, 1H, –NH^{a}CO–), 6.37 (d, 1H, J=8.2 Hz, –NH^{b}CO–), 7.02—7.33 (m, 10H, Ar-H), 7.80 (d, 1H, J=7.3 Hz, –NH^{c}CO–); ^{13}C-NMR ($CDCl_3$) ppm 14.13 (Me), 21.24 (Leu Me), 22.69 (Leu Me), 23.27 (C10, 11), 24.71 (C9), 26.82 (Leu C$^{\gamma}$), 29.22 (C8), 29.31 (C7), 29.35 (C6), 29.56 (C5), 29.64 (C4), 29.67 (C3), 31.92 (C2), 37.10 (Phe^1 C$^{\beta}$), 37.59 (C1), 39.64 (Phe^2 C$^{\beta}$), 43.41 (Leu C$^{\beta}$), 53,14 (Leu C$^{\alpha}$), 53.76 (Phe^2 C$^{\alpha}$), 54.29 (Phe^1 C$^{\alpha}$), 126.77 (*p*), 127.13 (*p*), 128.50 (*o*), 128.70 (*o*), 129.28 (*m*), 129.40 (*m*), 136.39 (*i*), 136.62 (*i'*), 170.00 (–NH^{a}CO–), 170.54 (–NH^{b}CO–), 176.31 (–NH^{c}CO–); FAB-MS (nitrobenzyl alchohol) *m/z* 593 (M^++1).

CD Measurements The CD spectra of **8a**—**d**—**10a**—**h** and **19a** were measured on a JASCO J-720 spectrophotometer. Measurements were made in a 1 cm path length in 85% methanol, circular quartz cell at ambient temperature. The CD spectra are shown in Figs. 3—5 with molar ellipticity, [θ], *versus* wavelength, λ(nm).

^{1}H-NMR Titrations All ^{1}H-NMR titration were run at 296 K. ^{1}H-NMR spectra were taken for each tube and δ values were calculated by substracting the chemical shift (δ_x) of interest in the spectrum of the mixtures from two α protons (-Phe^1 C$^{\alpha}$H, -Phe^2 C$^{\alpha}$H) and two-three amido protons (δ_0) (–NH^{a}CO–, –NH^{b}CO–, or –NH^{c}CO–) in the spectrum of double-stranded peptides **8a**, **8e**, **8f**, **10a**, **10g**, **14a**, **14b**, and **16a** in $CDCl_3$. In 2 separate NMR tubes 9.0 mg of **8a** and 1.0/0 and 0.5 ml/0.2 ml of the mixture solution of $CDCl_3$ and DMSO-d_6 were added. Concentration ranges for the NMR titrations are as follows: (a) In **8a**, [**8a**]=1.63×10^{-2} M. (b) In **8e** and **8f**, [**8e**, **f**]=1.60×10^{-2} M. (c) In **10a**, **14a**—**b**, and **16a**, [**10a**], [**14a**—**b**], [**16a**]=1.0−1.27×10^{-2} M.

Binding Studies UV data were collected on a JASCO U-best 30 spectrophotometer in a 10 mm quartz cell in methanol. The value of association constant (K_a) was the average of the mean values obtained in the evaluation of the three individual 1 (nm). The concentrations of double-stranded peptides, **8a**, **8b**, **10a**, and **10c**, varied as follows: In **8a** and pyrene, [pyrene]=6.625×10^{-6} M. [**8a**]=0.0, 0.496, 0.992, 1.98, 3.97, 5.96, 7.94 (×10^{-4} M). In **8b** and azobenzene, [azobenzene]=2.11×10^{-5} M. [**8b**]=0.0, 0.998, 9.98, 59.9 (×10^{-5} M). In **10a** and azobenzene, [azobenzene]=1.758×10^{-5} M. [**8b**]=0.0, 0.129, 0.259, 0.648, 1.29, 1.943(×10^{-3} M). In **10c** and PHA, [PHA]=8.05×10^{-5} M, [**10c**]=0.0, 0.955, 1.91, 3.82, 9.55, 19.09 (×10^{-4} M). In **14a** and azobenzene, [azobenzene]=2.857×10^{-5} M, [**14a**]=0.0, 0.868, 3.47, 8.68, 13.02 (×10^{-4} M). In **16a** and azobenzene, [azobenzene]=2.857×10^{-5} M, [**16a**]=0.0, 0.135, 2.70, 8.10, 13.50 (×10^{-4} M).

Energy Calculation The energy calculations were performed by using the CS software with MM2 to determine a minimum energy conformation (local minimum) of mini double-stranded peptides, and by assuming fixed dihedral angle (∠C5–C6–C7–C8, θ (degree)) in dodecano spacer.

Acknowlegements This work was supported by a part of Special Coordination Funds from the Science and Technology Agency(Japan).

References and Notes

1) *a*) Mutter M., *Angew. Chem. Int. Ed. Engl.*, **24**, 639—653 (1985); *b*) Sibanda B. L., Blundel T. L., Thornton J. M., *J. Mol. Biol.*, **206**, 759—777 (1989); *c*) Creighton T. E., "Proteins: Structures and Molecular Principle," 2nd ed., Freeman W. H. and Co., New York, 1993; *d*) Ramirez-Alvarado M., Kortemme T., Blanco F. J., Serrano L., *Bioorg. Med. Chem.*, **7**, 93—103 (1999).
2) *a*) Suzuki M., *J. Mol. Biol.*, **207**, 61—84 (1990); *b*) Harding M. M., *J. Med. Chem.*, **35**, 4658—4664 (1992).
3) *a*) Barrow C. J., Yasuda A., Kenny P. T., Zagorski M. G., *J. Mol. Biol.*, **225**, 1075—1093 (1992); *b*) Sticht H., Bayer P., Willbold D., Dammes S., Hilbich C., Beyreuther K., Frank R. W., Rosch P., *Eur. J. Biochem.*, **233**, 293—298 (1995).
4) *a*) Somers W. S., Philips S. E. V., *Nature* (London) **359**, 387—393 (1992); *b*) Maynard A. J., Searle M. S., *Chem. Commun.*, **1997**, 1297—1298.
5) Ovchinnikov Y. A., Ivanov V. T., *Tetrahedron*, **31**, 2177—2209 (1975).
6) *a*) Hopkins R. B., Hamilton A. D., *J. Chem. Soc., Chem. Commun.*, **1987**, 171—173; *b*) Diaz H., Tsang K. Y., Choo D., Espina J. R., Kelly J. W., *J. Am. Chem. Soc.*, **118**, 3790—3791 (1996); *c*) Nowick J. S., Holmes D. L., Mackin G., Noronha G., Shaka A. J., Smith E. M., *ibid.*, **118**, 2764—2765 (1996); *d*) Austin R. E., Maplestone R. A., Sefler A. M., Liu K., Hruzewicz W. N., Liu C. W., Cho H. S., Wemmer D. E., Bartlett P. A., *ibid.*, **119**, 6461—6472 (1997); *e*) Raghothama S. R., Awasthi S. K., Balaram P., *J. Chem. Soc., Perkin Trans. 2*, **1998**, 137—143.
7) The steric energy calculations were performed using the CS Chem 3D pro with MM2 force field. Allinger N. L., *J. Comput. Chem.*, **14**, 755—768 (1993).
8) Anderson G. W., Paul R., *J. Am. Chem. Soc.*, **80**, 4423 (1958).
9) Takuma S., Hamada Y., Shioiri T., *Chem. Pharm. Bull.*, **30**, 3147—

3153 (1982).
10) *a*) Bandekar J., Evans D. J., Krimm S., Leach S. J., Lee S., McQuie J. R., Minasian E., Nemethy E., Pottle M. S., Scheraga H. A., Stimson E. R., Woody R. W., *Int. J. Pept. Protein Res.*, **19**, 187—205 (1982); *b*) Woody R. W., *Meth. Enzymol.*, **246**, 34—71 (1995).
11) *a*) Blout E. R., Schmier I., Simmons N. S., *J. Am. Chem. Soc.*, **84**, 3193—3194 (1962); *b*) Bush C. A., Sarkar S. K.,Kopple K. D., *Biochemistry*, **17**, 4951—4954 (1978); *c*) Akamatsu M., Fujita T., *J. Pharm. Sci.*, **81**, 164—173 (1992).
12) Raghothama S, Chaddha M, Balaram P., *J. Phys. Chem.*, **100**, 19666—19671 (1996).
13) Bour P., *J. Phys. Chem. A*, **103**, 5099—5104 (1999).
14) Sheinerman F. B. and Brooks C. L., *J. Am. Chem. Soc.*, **117**, 10098—10103 (1995).
15) Hoch J. C., Dodson C. M., Karplus M., *Biochemistry*, **24**, 3831—3841 (1985).
16) The corresponding ϕ- and ω-angles (degree) were calculated from the equation $^3J_{\alpha N}=6.4\cos\theta-1.4\cos\theta+1.9$ ($\theta=\phi-60$).[15)]
17) 1,2-Ethano-bis(D-Leu) gave crystals suitable for X-ray analysis. Crystallographic analysis; cell constants and an orientation matrix for data collection corresponded to a primitive orthorhombic cell with dimensions: $a=11.375$ Å, $b=15.857$ Å, $c=9.761$ Å, and $V=1760.6400$ Å^3.
18) Wuthrich K., "NMR of Proteins and Nucleic Acids," John Wiley and Sons, New York, 1986.
19) Nagakura S., *J. Am. Chem. Soc.*, **76**, 3070—3073 (1954).